Macromolecules

pubs.acs.org/Macromolecules Article

Exploring Isomeric Effects on Optical and Electrochemical Properties of Red/Orange Electrochromic Polymers

Graham S. Collier, Riley Wilkins, Aimée L. Tomlinson, and John R. Reynolds*

Cite This: *Macromolecules* 2021, 54, 1677−1692 Read Online

ACCESS | Metrics & More | Article Recommendations | Supporting Information

ABSTRACT: Subtle structural changes in monomeric building blocks can have an immense effect, whether positive or detrimental, on the resulting properties of conjugated polymers. With this in mind, it is paramount to understand structure−property relationships that serve as the guiding principles for manipulating optical and electrochemical characteristics. Herein, a family of dialkylthiophene-*co*-propylenedioxythiophene copolymers are synthesized via direct arylation polymerizations, with a key design motif being minimal changes in the structural composition of the propylenedioxythiophene comonomer. Variation in the substitution pattern on the propylene bridge provides insights into the role of stereo- and compositional isomers on the resulting polymer properties. Specifically, time-dependent density functional theory calculations reveal changes in the number and placement of comonomers with varying composition and stereocenters, impacting the calculated absorbance spectra, as evident from calculated absorbance maxima spanning 75 nm, which ultimately manifests in differences in the calculated color. Experimentally, UV−vis absorbance spectroscopy and colorimetry reveal a dependence on the stereo- and regiospecificity, while electrochromic properties, such as contrast and switching times, are not drastically affected by the substitution patterns. Independent of position and functionality, each polymer exhibited a transmittance change greater than 65% at the maximum absorbance wavelength while maintaining the ability to rapidly switch between colored and transmissive states in organic electrolytes. This work highlights how subtle structural changes can manipulate and optimize optical features without sacrificing electrochromic properties such as kinetic switching time and optical contrast. In addition to fundamental insights into monomeric design of propylenedioxythiophene building blocks and their optical and redox characteristics, the results provide an additional structural handle for fine-tuning the observed color of electrochromic polymers.

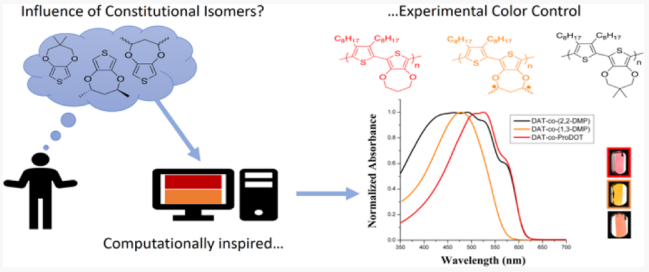

INTRODUCTION

Conjugated polymers find utility in redox-active applications,[1−3] such as electrochromism[4,5] and bioelectronics,[6] due to the ability to readily manipulate their properties and processability through synthetic design. For example, when considering electrochromism, full color control is possible by balancing electronic and steric contributions from comonomers and their respective side chains.[7] Additionally, broadly absorbing electrochromic polymers (ECPs) can be synthesized to access various shades of black electrochromic films using the donor−acceptor approach[8−13] or different hues across the color palette using all-thiophene terpolymers.[14] While robust structure−property relationships that enable accurate color control have been established, high-gap ECPs with optical absorbances between 380 and 550 nm to produce films in the yellow−orange−red color space are still a significant challenge for the field. Tailoring polymer structures that absorb in the high-gap region of the visible spectrum is challenging due to the difficulty in balancing desired optical features with electrochemical properties. High-gap ECPs are desirable from a practical point of view due to their utility as components of subtractive color mixing ECP blends to access various secondary colors around the color palette or blacks and browns via coprocessing.[15−21] One major limitation for these blends is the long-term switching stability between colored and transmissive states due to the instability of chemical structures that absorb in this region of the visible spectrum. Therefore, it is necessary to establish effective design strategies for synthesizing electrochemically stable high-gap ECPs.

Historically, triphenylamine-type comonomers have been shown to be suitable building blocks to access optical absorbance profiles that yield yellow electrochromic films. The resulting copolymers suffer from having high oxidation potentials and difficulty reaching a fully transmissive state upon oxidation due to the disruption of conjugation by the nitrogen lone pair of electrons.[22−25] Efforts from both Sotzing and co-

Received: December 8, 2020
Revised: January 21, 2021
Published: February 5, 2021

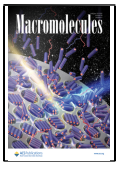

https://dx.doi.org/10.1021/acs.macromol.0c02719
Macromolecules 2021, 54, 1677−1692

Scheme 1. Representative Schematic Detailing Polymer Structures Studied in This Work and Illustrating the Scope of Structure−property Relationships Explored

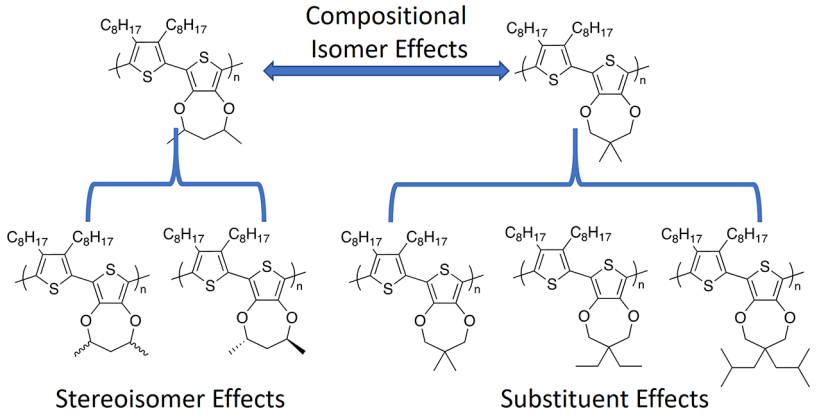

workers, and our group, have involved utilizing redox-active dioxythiophenes as an alternative design strategy. Sotzing's strategy consisted of varying substituent identity at the 1- and 3-positions of the propylene bridge of 3,4-propylenedioxythiophene (ProDOT) as a means to manipulate the steric contributions that enables full visible spectrum tuning and subsequently the final color of electropolymerized homopolymers.[26,27] Our group's approach involved developing a solution-processable copolymer synthesized via palladium-catalyzed Suzuki cross-coupling polymerizations using ProDOT and phenylene comonomers (ProDOT-Ph).[28] This polymer has a maximum absorbance (λ_{max}) of 455 nm and the ability to rapidly switch between colored to transmissive states. However, while this copolymer possessed the necessary optical properties, ProDOT-Ph had a relatively high oxidation potential of 1.1 V versus Ag/Ag^+ due to the increased aromaticity of the phenylene comonomer compared to dioxythiophene. The high oxidation potential, in combination with accessible reactive sites on the unsubstituted phenylene comonomer, led to poor redox stability after 10−20 redox cycles. In an effort to circumvent these stability issues while achieving a transmissive oxidized state, yellow ECPs were further developed by using various arylene comonomers and methoxy-substituted phenylene building blocks.[29−31] Introducing the electron-donating groups on the arylene units yielded high-gap copolymers with lower oxidation potentials and led to a slight increase in redox stability. Specifically, the redox stability of films improved by withstanding degradation for more than 100 cycles compared to the 10−20 cycles observed for PProDOT-Ph. However, increasing the stability of these high-gap systems beyond 100 redox cycles is still paramount due to the superior redox stability of other ECPs that are used in blending studies. Overcoming limitations of redox stability of yellow ECP sets the precedent to explore different polymer structures and synthesize high-gap ECPs without phenylene-based comonomers.[32]

An alternative strategy for accessing high-gap ECPs involved utilizing acyclic dioxythiophene polymers (PAcDOTs) that were functionalized with branched alkoxy solubilizing chains and copolymerized with 3,4-dimethoxythiophene or ethylenedioxythiophene.[33−35] The PAcDOT-based polymers represented a new class of orange and red ECPs that exhibit λ_{max} values between 485 and 525 nm while maintaining relatively low onsets of oxidation due to the electron-donating nature of the oxygen atom adjacent to the thiophene backbone. This work was advantageous beyond the seminal work on red electrochromics based on substituted thiophenes[36] and has since motivated other research groups to realize diverse strategies to access conjugated polymers in the same color space, culminating in red ECPs being synthesized with benzotriazole,[37] phenanthrocarbazole,[38] indacenodithiophene,[12,39] and thienothiophene[40] building blocks. However, these systems suffer from poor electrochromic contrast or exhibit colored-to-colored electrochromic properties and are not suited for transmissive electrochromic applications. More recently, our group synthesized a family of copolymers utilizing a dialkylthiophene (DAT) comonomer coupled with various dioxythiophene comonomers.[41] DAT-based copolymers represent the first family of high-gap ECPs without utilizing phenylene-based comonomers, while also possessing improved redox stability, as evident by minimal changes in contrast over 1000 redox cycles. The octyl-solubilizing side chains on the DAT comonomer provided the intraring strain required to absorb ∼350 to ∼600 nm and protected the polymer backbone from undesired side reactions, while the dioxythiophene comonomers provided adequate redox activity to switch the polymers at low oxidation potentials (<1.0 V vs Ag/Ag^+). Ultimately, various orange- and red-to-transmissive ECPs were obtained, highlighting the ability to access various hues in the high-gap color space using this design strategy. Considering these successes, we are motivated to further explore the ability to fine-tune optical and color properties of high-gap ECPs.

In thinking of effective design strategies for high-gap ECPs, the concept of probing isomeric effects comes to mind due to the ability to readily introduce compositional and stereoisomer comonomers into the polymer repeat unit, as illustrated by the repeat unit structures in Scheme 1. Motivated by the successes realized by our group, and by Sotzing and co-workers, using 1,3-ProDOTs, we were intrigued to further understand how subtle changes in comonomer structures, specifically the role of stereo- and compositional isomers, can be further exploited to fine-tune optical and electrochemical properties of high-gap ECPs. The desire to investigate isomer effects on redox-active copolymers is further motivated by extensive work on manipulating the backbone and side-chain structures of conjugated polymers used for myriad applications, such as organic field effect transistors, organic photovoltaics, and sensing applications.[42−61] With respect to dioxythiophenes, stereo- and regio-specificity is less understood, but preliminary studies indicate these structural features should not be

https://dx.doi.org/10.1021/acs.macromol.0c02719
Macromolecules 2021, 54, 1677−1692

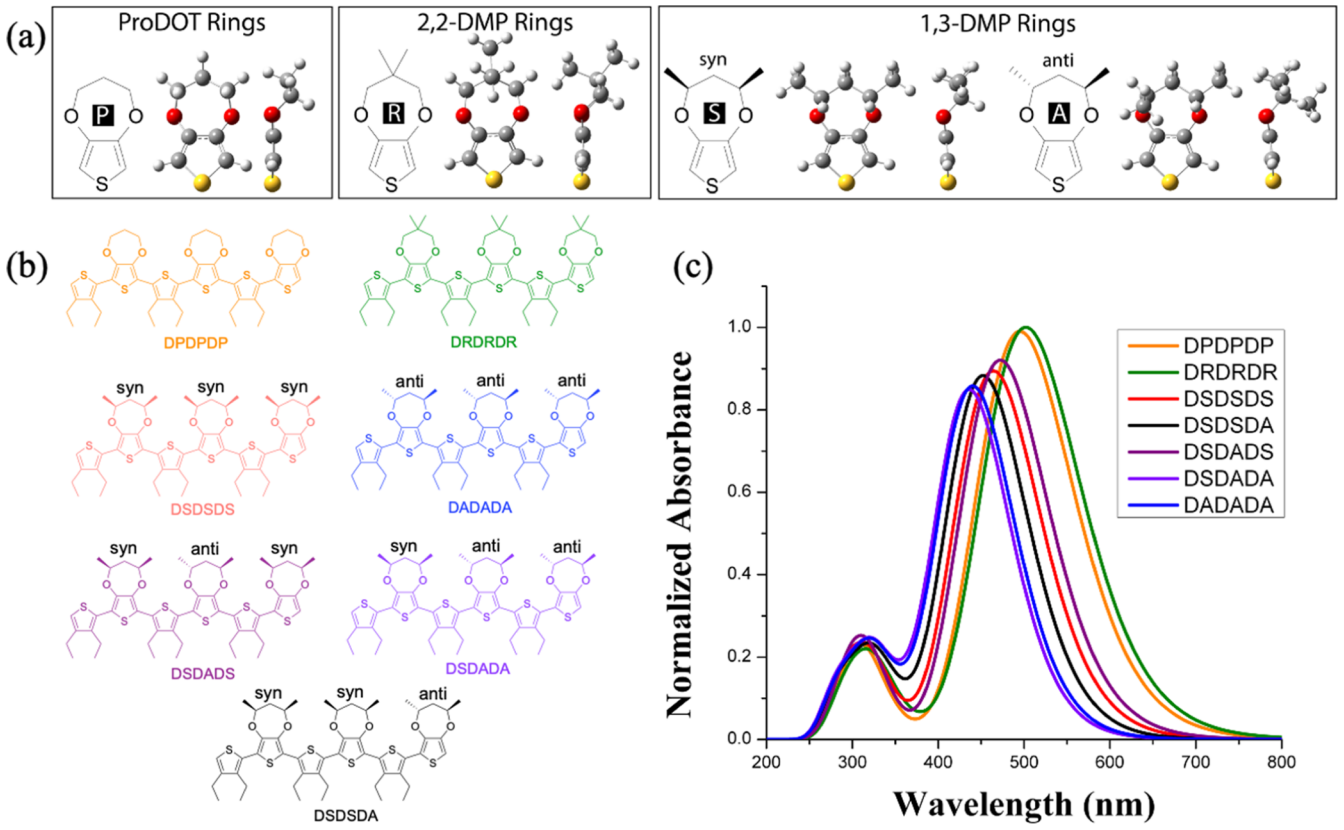

Figure 1. Aryl group legend (a) and seven oligomers (b) composed of six aryl rings are provided to elucidate compositional, regio-, and stereoisomerism on UV−vis spectral properties. The neutral UV−vis spectra resulting from TD-DFT calculations for the seven structures are shown in (c).

forsaken. Bäuerle and co-workers demonstrated that fully stereoregular poly(EDOTs), synthesized via electrochemical polymerization, possessed improved interchain interactions and lower onsets of oxidation. However, a thorough investigation into these effects on optical properties was not performed.[62,63] In another study published as this manuscript was being drafted, Gidron and co-workers demonstrated the use of electronic circular dichroism as an analytical technique that provides insights into chiroptic properties and film morphology that is dependent on electrochemical conditions.[64] Regiospecificity is known to be a useful design strategy to influence solution and solid-state properties of dioxythiophene polymers. This dependence was demonstrated by a phenylenedioxythiophene homopolymer that exhibits significant inter- and intrachain interactions in solution and the solid-state that lead to well-defined 2D self-assembled nanostructures.[65] Furthermore, ProDOT possesses a *C*2 symmetry, which allows for regiosymmetric polymers to be synthesized with new optical and electrochemical properties compared to poly(EDOTs).[66,67] Considering the structural diversity envisioned for functionalizing ProDOTs[68,69] at various positions of the propylene bridge, there is a precedent to elucidate isomeric effects on structure−property-relationships of high-gap ECPs.

Along these lines, herein, we correlate stereo- and compositional isomeric effects on the optical and electrochemical properties of high-gap ECPs by combining experimental and theoretical approaches. By changing methyl-substitution patterns from the 1,3-positions to the 2,2-positions of the propylene bridge of a ProDOT comonomer, the UV−vis absorbance of the resulting films evolve from featureless absorbance profiles for the 1,3-ProDOT copolymers to spectra with absorbances spanning >200 nm in breadth with fine-structure features at longer wavelengths for the 2,2-ProDOT copolymers. Structural intricacies are further probed by synthesizing a stereospecific 1,3-dimethylProDOT comonomer that is incorporated into a DAT-*co*-ProDOT copolymer. Upon characterization, introducing stereospecificity to the polymer backbone induces surprising electromagnetic shielding effects in ^{1}H NMR spectra, measurable differences in the UV−vis absorbance spectra of thin films, and quantifiable differences in the resulting colorimetry. A family of 2,2-ProDOTs is synthesized, where the functionality was varied by methyl, ethyl, and isobutyl substituents, and is successfully incorporated into DAT-based copolymers. Each of these polymers display significant broadening and increased fine-structure absorbance features in their UV−vis absorbance spectra after electrochemical conditioning, which translates to the neutral polymers possessing hues of red. While the minimal structural changes at the 2,2-positions did not drastically influence the absorbance profiles or the color of the resulting films, increasing the bulkiness of the substituent increased the propensity of the film to maintain its red hue after repeated electrochemical switching. Ultimately, this study demonstrates the importance of understanding polymer properties as a function of the structure by highlighting how subtle differences of compositional isomers within a polymer backbone influences fundamental structural, optical, and color properties.

https://dx.doi.org/10.1021/acs.macromol.0c02719
Macromolecules 2021, 54, 1677−1692

RESULTS AND DISCUSSION

To elucidate the influence that compositional isomers have on the excited state transitions of the resulting alternating copolymers, time-dependent density functional theory (TD-DFT) calculations were performed. The mPW1PBE functional paired with the cc-PVDZ basis set on model systems possessing 6 aryl groups have proven to accurately correlate calculated and experimental absorbance spectra, as well as the resulting color of ECPs.[70] The impact of substituent number, location and orientation on spectra, and therefore color, was examined by choosing seven oligomers using the legend provided in Figure 1a. Here, P = ProDOT, R = regiosymetric 2,2-dimethylProDOT, and S = 1,3-dimethylProDOT with the methyl groups possessing the same stereochemical relationship with respect to the dioxythiophene reference plane (i.e., syn). Alternatively, A = 1,3-dimethylProDOT with an alternating stereochemical relationship (i.e., anti) that represents a mixture of R,R and S,S stereoisomers at the 1,3-position of the propylene bridge. Systems possessing diethylthiophene (D) rings that are alternated with only ProDOT (DPDPDP) and 2,2-DMP (DRDRDR) rings were compared to those paired with variations of the two 1,3-DMP isomers (DSDSDS, DSDSDA, DSDADS, DSDADA, and DADADA) (Figure 1c). For each system, the neutral and radical cation geometries were optimized and the frequency was verified. The UV−vis spectra and the predicted color were generated through a TD-DFT computation (using mPW1PBE/cc-PVDZ) to find the lowest lying 15 excited states for both neutral and radical cation forms. A comparison between DPDPDP and DRDRDR versus the other five systems resulted in band gap and aryl ring dihedral angle variances of 0.37 eV and 39°, respectively. (See Figure S1 for the dihedral angle legend and Table S1 for corresponding data). These differences impacted both the simulated spectra as well as the predicted color for the different systems (Figure 1c and Table S1). The DPDPDP and DRDRDR oligomers possessed λ_{max} of 495 and 502 nm, respectively, and indistinguishable oscillator strengths (f) (1.94 for DPDPDP and 1.95 for DRDRDR) culminating in nearly identical spectra and color for these species (see Table S3 and Figure 1). The remaining systems were blue-shifted and possessed a λ_{max} and f range from 427 to 464 nm and 1.65 to 1.80, respectively, thereby giving predicted color differences with various orange hues. Unlike the neutral species, the radical cation set possessed λ_{max} and f deviations of 26 nm and 0.32 (see Table S4), producing comparable simulated spectra in the visible range. These similarities led to only slight color differences between the seven oligomers (see Table S2). Calculations support the hypothesis that stereo- and regiospecificity will influence the optical properties and subsequently, the color of neutral polymers, while minimal change is produced for the radical cation set. Specifically, the observed blue-shifts in the calculated absorbance spectra of each 1,3-ProDOT hexamer motivated our synthetic efforts to elucidate subtle differences in neutral colors.

Having identified regio- and stereospecific synthetic targets from our theoretical studies, we began the process of synthesizing and characterizing monomers and copolymers to combine experimental and computational results. ProDOT and DAT comonomers were prepared following our previously developed synthetic protocols.[71] First, ProDOT monomers were synthesized via transetherfication reactions between 3,4-methoxythiophene and the corresponding diol in the presence of p-toluenesulfonic acid in refluxing toluene. Notably, yields for 2,2-substituted ProDOTs were higher (46−67%) compared to those of 1,3-dimethyl ProDOTs (∼20%) due to the different steric contributions during the ring closing. Synthesis of the dialkyl-thiophene comonomer was accomplished following the Kumada cross-coupling procedure reported for the first generation of DAT electrochromic copolymers.[41] Detailed procedures, methods, and structural characterization can be found in the Supporting Information (Figures S2−S7).

Palladium-catalyzed direct heteroarylation polymerization (DHAP) conditions previously used to synthesize electron-rich ECPs were followed for the synthesis of each DAT-*co*-ProDOT copolymer.[72−74] Polymerizations were performed in *N*,*N*-dimethylacetamide at 140 °C using palladium(II) acetate ($Pd(OAc)_2$) as the catalyst, potassium carbonate (K_2CO_3) as the base, and pivalic acid (PivOH) as the proton shuttle. It is worth noting that attempts using 3,4-bis(octyl)thiophene as the dihydro comonomer yielded an oligomeric material with number-average molecular weights (M_n) ∼4.0−7.0 kg/mol as measured via size-exclusion chromatography (SEC) versus polystyrene (PS) standards. Historically, dioxythiophene-based copolymers with M_n values below 10.0 kg/mol neither exhibit sufficient film forming properties during processing for materials with robust redox switching, nor are the polymers in their limit of conjugation length as needed for saturated electronic properties.[75] This motivated the use of Br_2-DAT as the dibromo comonomer for polymerization protocols, as shown in Scheme 2. By switching monomer functionality and

Scheme 2. Direct Arylation Polymerizations of Various ProDOT Comonomers Using a Dibrominated DAT Comonomer

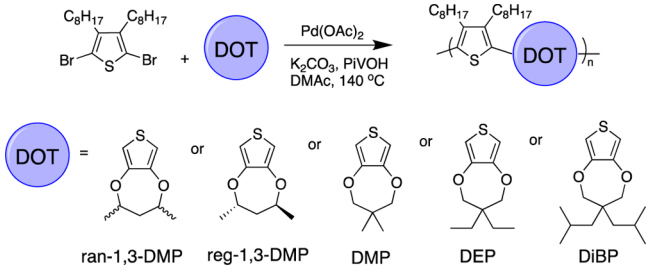

the corresponding sequence of participation in the DHAP catalytic cycle, copolymers using the respective ProDOT as dihydro comonomers were successfully synthesized. All of the copolymers were isolated in excellent yields (>80%) with similar M_n (20−30 kg/mol) and dispersities ($Đ$ = 2.1−3.6) as measured by SEC (Figure S8) and are reported in Table 1. Additionally, as tabulated in Table 1, elemental analyses reveal each copolymer is obtained with high compositional purity, which is necessary to establish accurate structure−property relationships.[76−81]

Stereoisomer Effects. Structural differences induced by the stereospecificity of 1,3-dimethylProDOTs were investigated using ^{1}H NMR, and the resulting spectra are illustrated in Figure 2. Notably, distinct changes in the chemical shifts and splitting patterns of stereorandom (black trace) and stereospecific (red trace) monomers are measured. The difference in chemical shifts for the protons immediately adjacent to the ProDOT oxygens (4.0 vs 4.4 ppm for the stereorandom and stereospecific monomers, respectively) is a result of the protons being more deshielded in the stereospecific monomer

https://dx.doi.org/10.1021/acs.macromol.0c02719
Macromolecules 2021, 54, 1677−1692

Table 1. Physical Properties and Elemental Purities of DAT-ProDOT Copolymers

				elemental analysis		
				actual (theoretical)		
polymer	yield (%)	M_n (kg/mol)	M_w/M_n ($Đ$)	C (%)	H (%)	S (%)
DAT-*co*-(ran-1,3-DMP)	83	18.3	2.1	71.27 (70.97)	9.04 (9.45)	13.05 (13.06)
DAT-*co*-(reg-1,3-DMP)	92	29.1	2.4	71.11 (70.97)	9.37 (9.45)	12.98 (13.06)
DAT-*co*-(DMP)	83	18.1	2.1	70.70 (70.97)	8.98 (9.45)	13.04 (13.06)
DAT-*co*-(DEP)	87	19.9	2.7	71.79 (71.76)	9.54 (9.71)	12.29 (12.36)
DAT-*co*-(D*i*BP)	87	19.6	3.6	73.06 (73.11)	10.07 (10.17)	11.05 (11.15)

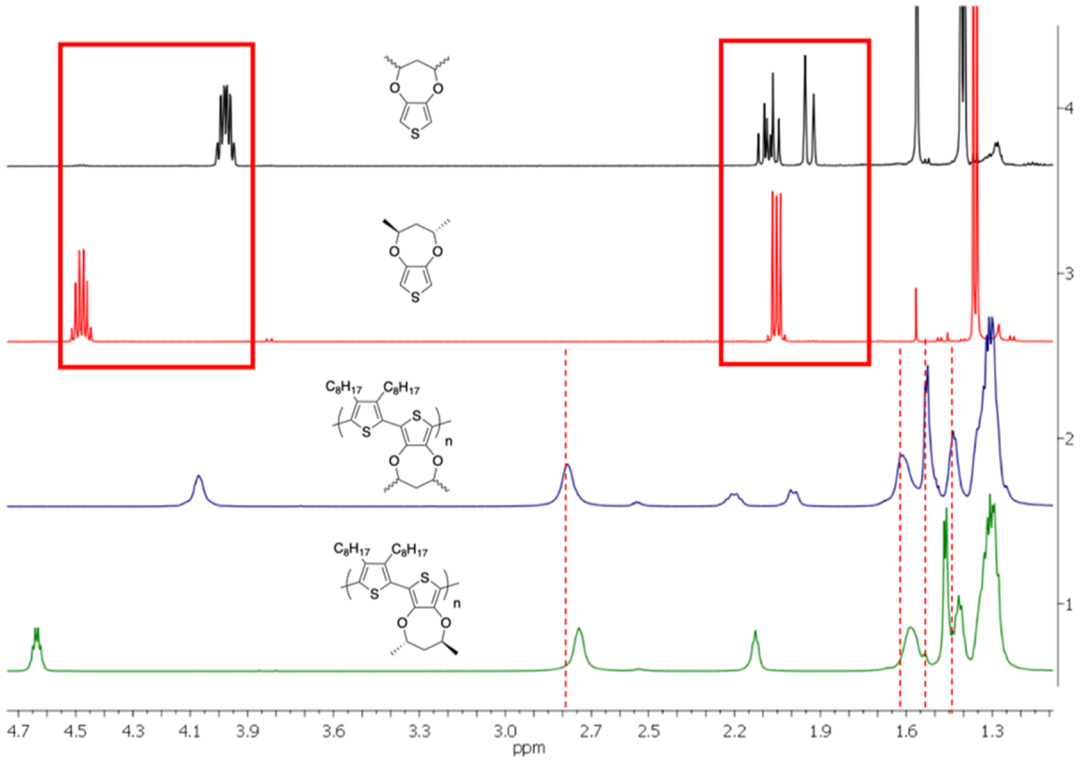

Figure 2. Overlaid ^{1}H NMR spectra of (black) stereorandom 1,3-dimethylProDOT, (red) stereospecific 1,3-dimethylProDOT, (blue) DAT-*co*-(ran-1,3-DMP), and (green) DAT-*co*-(reg-1,3-DMP) measured in $CDCl_3$ at 25 °C. The red box 1.8 ppm < δ < 2.2 ppm and the red box 3.9 < δ < 4.6 ppm highlight stereospecificity shielding and coupling effects in the ProDOT monomers while the red dashed lines emphasize the changes in shielding effects on the alkyl solubilizing chains in the resulting copolymers.

compared to the stereorandom monomer. Chemical shifts ~2.0 ppm correspond to protons at the 2,2-position of the propylene bridge. The peaks corresponding to a mixture of stereoisomers in the black trace transition to a single multiplet in the red trace, which confirms the retention of stereocenters during the etherification reaction. When these monomers are incorporated into copolymers to construct DAT-*co*-(ran-1,3-DMP) (blue trace) and DAT-*co*-(reg-1,3-DMP) (green trace), the stereospecific comonomer increases electromagnetic shielding of protons on the DAT-solubilizing side-chains, which leads to an upfield shift relative to the copolymer synthesized with the stereorandom comonomer. These changes in chemical shifts demonstrate that stereospecificity influences fundamental structural features of the resulting copolymers and provides the motivation to further probe these effects on macromolecular properties.

UV−vis absorbance spectra of DAT-*co*-(ran-1,3-DMP) and DAT-*co*-(reg-1,3-DMP) dissolved in toluene were measured to experimentally explore the effects of stereospecificity on polymer optical properties. As depicted in Figure 3a, the solution UV−vis absorbance profiles of both 1,3-DMP copolymers are identical with maximum absorbances (λ_{max}) at 440 nm. The measured λ_{max} of the two synthesized 1,3-DMP copolymers is identical to the calculated λ_{max} of DADADA (440 nm), which represents DAT-*co*-(reg-1,3-DMP) and supports our level of theory. The observed changes in λ_{max} for other modeled oligomers compared to experimental measurements demonstrates how minor changes in the distribution of "stereorandomness" through the polymer backbone may influence electronic properties. Differential scanning calorimetry (DSC) was used to probe stereospecific effects on bulk thermal properties of each copolymer. As shown in Figure 3b, DAT-*co*-(ran-1,3-DMP) exhibits melting and crystallization transitions while DAT-*co*-(reg-1,3-DMP) does not. Previous work on poly(thiophenes) report that thermal transitions and solid-state architectures were dependent on the critical molecular weight (M_c) with the M_c of P3HT ≈ 25 kg/mol.[82] This molecular weight dependence was elucidated by observing a linear increase in the melting temperature (T_m) with increasing M_n, which is attributed to

https://dx.doi.org/10.1021/acs.macromol.0c02719
Macromolecules 2021, 54, 1677−1692

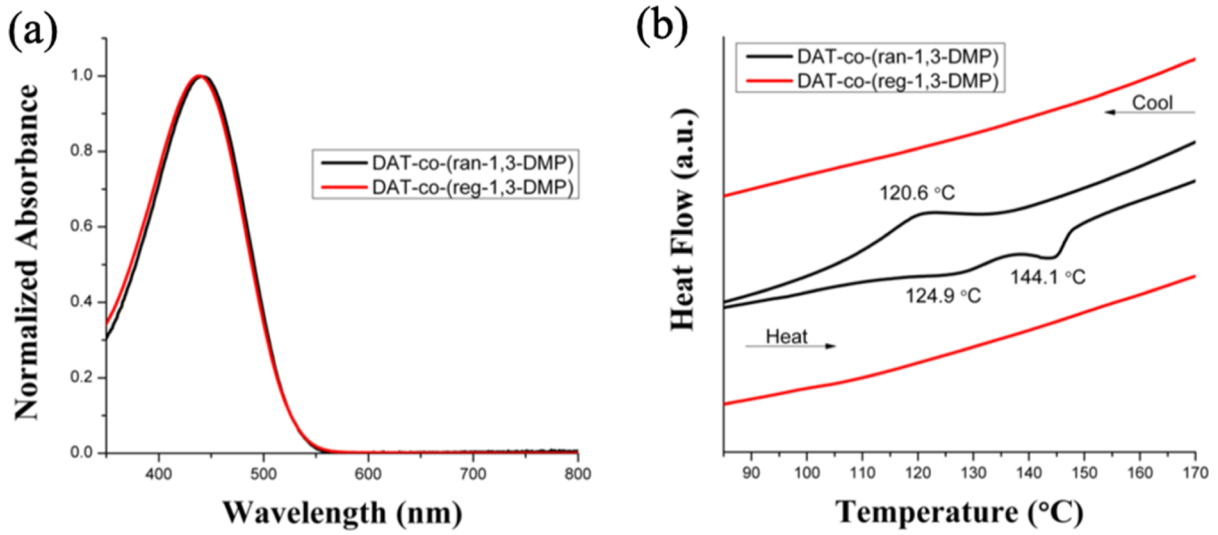

Figure 3. (a) Normalized solution UV−vis absorbance spectra of DAT-*co*-(ran-1,3-DMP) and DAT-*co*-(reg-1,3-DMP) dissolved in toluene with nominal concentrations of 15 μg/mL, and (b) differential scanning calorimetry traces of DAT-*co*-(ran-1,3-DMP) and DAT-*co*-(reg-1,3-DMP) (second heating cycle).

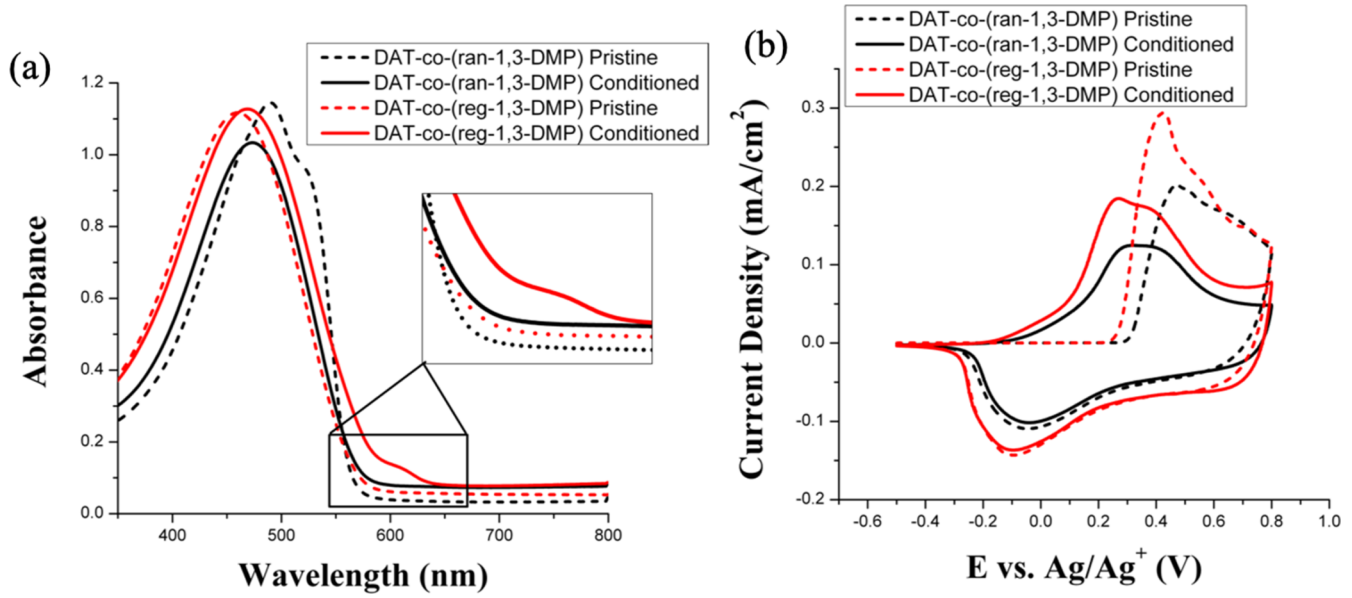

Figure 4. (a) UV−vis absorbance spectra and (b) cyclic voltammograms of pristine and electrochemically conditioned films of DAT-*co*-(ran-1,3-DMP) and DAT-*co*-(reg-1,3-DMP). UV−vis absorbance spectra were recorded by scanning from 350 to 800 nm. Electrochemical conditioning protocols consist of performing 10 CV cycles across a voltage window of −0.5 to 0.8 V (vs Ag/Ag^+ reference electrode) in a 0.5 M $TBAPF_6$/PC electrolyte solution using a scan rate of 100 mV/s.

the chain microstructure evolving from the ability to form chain-extended crystals to form interconnected "fringe-micelle" architectures. The differences in thermal properties exhibited by DAT-*co*-ProDOTs is believed to be related to the M_n and the ability of the copolymers to form crystalline domains. We speculate the observed transitions for DAT-*co*-(ran-1,3-DMP) (M_n = 18.3 kg/mol) may be attributed to the polymer's ability to form chain-extended crystals, while the amorphous nature of DAT-*co*-(reg-1,3-DMP) (M_n = 29.1 kg/mol) may indicate formation of "fringe-micelle" architectures. The thermal behavior suggests these copolymers possess a M_c between ∼18 and 30 kg/mol and is in agreement with the reported M_c of P3HT.[82] These results are fundamentally intriguing, and deeper structural studies are required to understand molecular weight effects on thermal and morphological properties of this family of copolymers.

To probe the effects of stereospecificity on optical properties in the solid state, UV−vis absorbance spectra were measured for films processed via spray-casting onto indium tin oxide (ITO) electrodes from toluene solutions with concentrations of 5 mg/mL. Films were sprayed to have transmittance (% T) values within 2% of each other in an effort to ensure accurate elucidation of structure−property relationships. UV−vis absorbance spectra of pristine and electrochemically conditioned films of DAT-*co*-(ran-1,3-DMP) and DAT-*co*-(reg-1,3-DMP) are shown in Figure 4a and Table 2. Analogous to differences in bulk thermal properties measured with DSC, UV−vis absorbance spectra of pristine films show distinct differences. First, DAT-*co*-(ran-1,3-DMP) as a pristine film is

https://dx.doi.org/10.1021/acs.macromol.0c02719
Macromolecules 2021, 54, 1677−1692

Table 2. Optical and Electrochemical Properties of Stereorandom and Stereospecific ProDOT Copolymers

polymer	λ_{max}^{soln} (nm)	λ_{max}^{film} (nm)	λ_{onset}^{film} (nm)	E_{onset}^{ox} (V)
DAT-*co*-(ran-1,3-DMP)	440	471	568	0.05
DAT-*co*-(reg-1,3-DMP)	440	470	590, (634)	−0.15

red-shifted compared to DAT-*co*-(reg-1,3-DMP) and also displays a vibronic fine-structure feature ∼525 nm, which is attributed to the more semicrystalline nature of the copolymer as observed in, and consistent with, DSC measurements. Alternatively, pristine films of DAT-*co*-(1,3-reg-DMP) exhibit broad, featureless absorbance profiles and have a blue-shifted absorbance maximum [∼450 vs ∼500 nm for DAT-*co*-(reg-1,3-DMP) and DAT-*co*-(ran-1,3-DMP), respectively]. Combined, the differences observed from DSC and UV−vis absorbance measurements support the notion of molecular weight dependence on polymer ordering in pristine films. For example, in our initial studies of DAT-based copolymers,[41] DAT-*co*-(ran-1,3-DMP) was synthesized with a M_n = 25.0 kg/mol (vs PS standards using $CHCl_3$ as the eluent) and displayed a broad, featureless absorbance profile. The broad, featureless absorbance spectrum is in contrast to DAT-*co*-(ran-1,3-DMP) synthesized for this study (M_n = 18.3 kg/mol) but analogous to DAT-*co*-(reg-1,3-DMP) (M_n = 29.1 kg/mol), which provides evidence that the polymers with $M_n \geq 25$ kg/mol are amorphous, while polymers below this molecular weight threshold have a minimal amount of order detectable with UV−vis spectroscopy.

After comparing the optical properties of the 1,3-DMP copolymers as pristine films, they were subjected to repeated redox reactions, known as electrochemical conditioning. This "electrochemical annealing" protocol is necessary as conjugated polymers often display changes in their redox response and absorbance features due to microstructural reorganization after doping and dedoping with exposure to solvent and ions.[83] Electrochemical conditioning protocols consist of performing 10 cyclic voltammetry (CV) cycles across a voltage window of −0.5 to 0.8 V (vs Ag/Ag^+ reference electrode) in a 0.5 M $TBAPF_6$/PC electrolyte solution using a scan rate of 100 mV/s. After conditioning, DAT-*co*-(ran-1,3-DMP) displays a blue-shift compared to the pristine film and the fine-structure feature is no longer visible. This blue shift suggests that the stereorandom copolymer becomes more disordered in the solid-state upon electrochemical annealing and agrees with our preliminary report on DAT-based copolymers.[41] Typically, the effective conjugation length of redox-active conjugated polymers is extended upon electrochemical conditioning and is ultimately accompanied with a red-shift in the absorbance spectrum.[66,67,84] Alternatively, after 10 CV cycles, the stereospecific copolymer DAT-*co*-(reg-1,3-DMP) exhibits a slight red-shift in the absorbance maximum and the evolution of a new transition at ∼600 nm is observed, ostensibly due to the evolution of aggregates. While there are noticeable differences in the absorbance profiles observed between pristine and conditioned films, absorbance maxima values are identical for DAT-*co*-(ran-1,3-DMP) and DAT-*co*-(reg-1,3-DMP) (see Table 2.). These findings highlight that while molecular weight may affect ordering and absorbance profiles of pristine films, electrochemical conditioning eliminates these influences. Cyclic voltammetric results in Figure 4b illustrates that after electrochemical conditioning DAT-*co*-(ran-1,3-DMP) has an onset of oxidation ∼0.0 V versus Ag/Ag^+ while the onset of oxidation for DAT-*co*-(reg-1,3-DMP) is ∼−0.1 V. These slight differences in the onset of oxidation, with the stereospecific copolymer displaying a slightly lower current onset, are consistent with the trends reported by Bäuerle indicating that ProDOT stereospecificity does influence the redox properties of these copolymers.[62] Specifically, the lower onset of oxidation of DAT-*co*-(reg-1,3-DMP), in addition to the red-shifted UV−vis absorbance spectrum after electrochemical annealing, indicates the stereospecific copolymers have improved interchain interactions compared to DAT-*co*-(ran-1,3-DMP).

The changes in absorbance as a function of electrochemical potential from −0.5 to 0.8 V were evaluated for electrochemically conditioned films of the stereorandom and stereospecific copolymers spray cast onto ITO electrodes from toluene. As shown in Figure 5, at ∼0−0.1 V, which corresponds to the onset of oxidation for the copolymers measured by CV, the

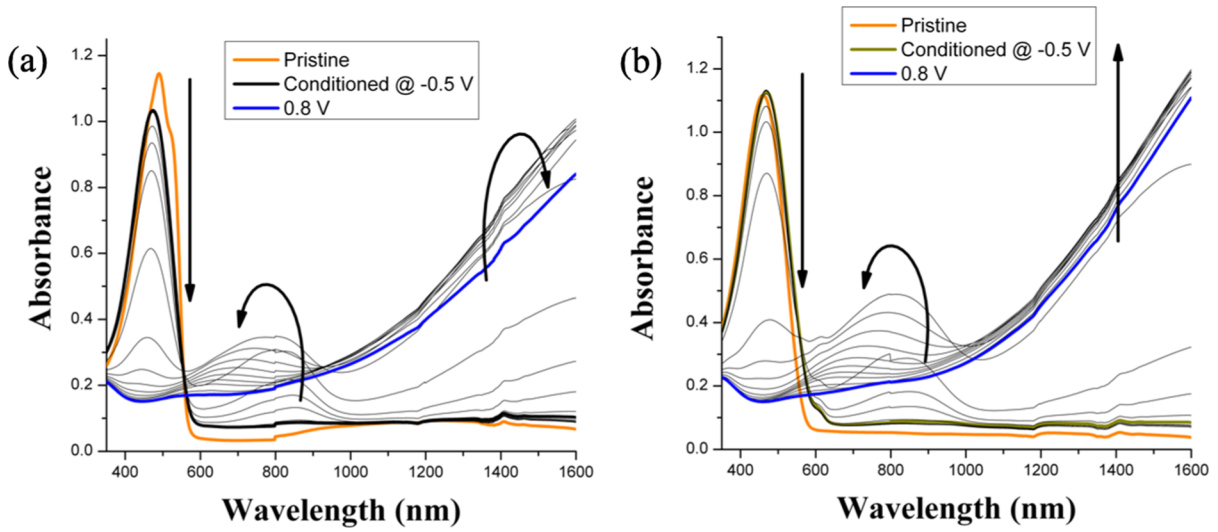

Figure 5. Absorbance spectra as a function of applied potential of (a) DAT-*co*-(ran-1,3-DMP) and (b) DAT-*co*-(reg-1,3-DMP) spray-cast from 5 mg/mL toluene solutions by applying 50 mV potential intervals from −0.5 to 0.8 V in 0.5 M $TBAPF_6$/PC electrolyte.

https://dx.doi.org/10.1021/acs.macromol.0c02719
Macromolecules 2021, 54, 1677−1692

neutral state absorbance in the visible region of the electromagnetic spectrum begins to decrease in intensity. This decrease in absorbance is accompanied with the formation of cation radicals (polarons) ~800 nm.[85,86] As the electrochemical potential is increased further, absorbance in the visible region and ~800 nm is depleted, while absorbance corresponding to the formation of dications (bipolarons) is observed beyond 1400 nm. These trends indicate that both copolymers transition from a vibrant orange film in the neutral state to a highly transmissive film when completely oxidized. Additionally, as shown in Figure 6, the absorbance intensity for

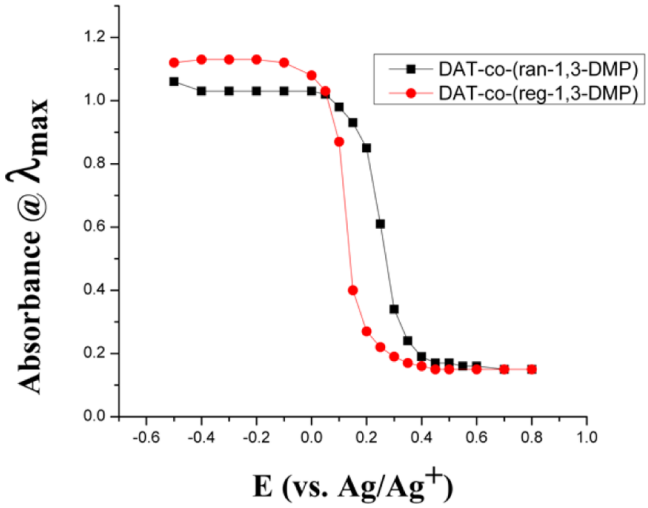

Figure 6. Absorbance at the wavelength of maximum absorbance versus electrochemical potential for DAT-*co*-(ran-1,3-DMP) and DAT-*co*-(reg-1,3-DMP).

DAT-*co*-(ran-1,3-DMP) and DAT-*co*-(reg-1,3-ProDOT) begins to diminish at their respective onsets of oxidation and demonstrate relatively uniform doping mechanisms with 50 mV increases in electrochemical potential. The steady depletion of absorbance observed in the spectroelectrochemical experiments indicates stereospecificity does not significantly influence steric interactions that impact nonplanar to planar transitions that occurs upon chemical doping.[33,87,88]

The differences observed in the UV−vis absorbance spectra ultimately influence the perceived color of the electrochromic films. Therefore, colorimetric analysis of the polymer films based on the "Commision Internationale de l'Eclairage 1976 $L^*a^*b^*$ color standards was used to quantify the effect of comonomer stereospecificity on the perceived color of DAT-*co*-(ran-1,3-DMP) and DAT-*co*-(reg-1,3-DMP). Colorimetry data illustrated in Figure 7 and tabulated in Table 3 indicate both copolymers fall in the orange color space and reach highly transmissive oxidized states with increasing electrochemical potential. In Figure 7, the color coordinates for the pristine films are identified by the circled data points, and upon electrochemical conditioning move to the points indicated by black arrows, and with continued 50 mV electrochemical steps, follow the path of the curved arrows tracking toward the graph's origin. Differences in the quantified color of the two copolymer films arise from slight variations in the a^* and L^* values. DAT-*co*-(reg-1,3-DMP) has a slightly larger a^* value (~33) compared to the a^* value measured for DAT-*co*-(ran-1,3-DMP) (~27). The measured color coordinates are in good agreement with DAT-*co*-(reg-1,3-DMP) having a slightly red-

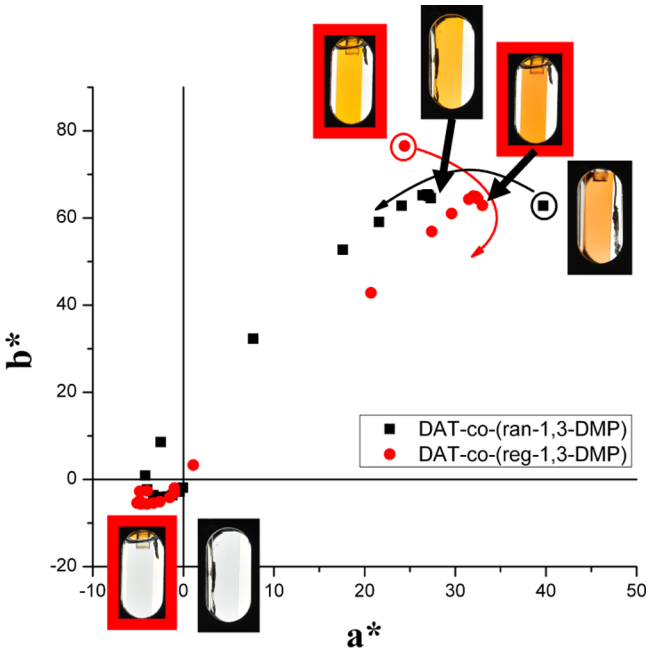

Figure 7. Color coordinates and photographs of DAT-(1,3-DMP) films spray cast from toluene obtained as a function of potential.

shifted absorbance spectrum compared to DAT-*co*-(ran-1,3-DMP) in Figure 4a, and thus, the film has a larger "red" component to the perceived color (i.e., larger a^*). As the electrochemical potential is increased and absorbance across the wavelength range 380−780 nm decreases, a^* and b^* values decrease and progress toward the plots' origin. The progression of the data across the third quadrant is a result of the tailing absorbance at longer wavelengths of the visible region before being depleted such that both copolymers demonstrate small a^* and b^* values (<-1 and ~2, respectively) as well as L^* values >85. Combined, these results indicate the polymers reach a highly transmissive, color-neutral oxidized state.

Redox and color stability of the DAT copolymers were performed by applying square-wave potential steps from −0.5 to 0.6 V versus Ag/Ag^+ to switch the films under an argon (Ar) atmosphere, where both copolymers demonstrate redox stability over the course of 500 switching cycles (Figure S9). It is important to note these experiments did demonstrate a dependence on the oxidizing potential. When voltages exceeded 0.6 V (vs Ag/Ag^+), significant film degradation (>50% of the optical contrast) was observed within 100 switching cycles. Interestingly, as shown in Figure 8a,b, the stereospecificity influences the long-term color stability. Here, color stability is defined as the ability of a polymer film to maintain its color after repeated electrochemical cycling and is calculated using the quantitative difference in color according to eq S1. Specifically, as shown in Figure 8a, DAT-*co*-(ran-1,3-DMP) exhibits only minimal change in the measured UV−vis absorbance spectrum after 500 redox cycles. Alternatively, DAT-*co*-(reg-1,3-DMP) (Figure 8b) shows a decrease in the $\pi-\pi^*$ transition, and the onset shoulder at ~600 nm continues to evolve. Changes in the absorbance spectra after extended electrochemical switching lead to differences in the quantitative difference in color, ΔE^*_{ab}, which is calculated according to eq S1. A ΔE^*_{ab} value larger than 2.3 means that two colors are noticeably different to the human eye. As shown in Table S5,

https://dx.doi.org/10.1021/acs.macromol.0c02719
Macromolecules 2021, 54, 1677−1692

Table 3. Electrochromic Properties of DAT-1,3-DMP Copolymers as Electrochemically Conditioned Films

	$L^*a^*b^*$					
polymer	neutral state	oxidized state	ΔT (%)	bleaching t_{95} (s)	coloration t_{95} (s)	τ (s)
DAT-*co*-(ran-1,3-DMP)	79, 27, 64	85, −0.5, −2	70	1.1	1.0	1.8
DAT-*co*-(reg-1,3-DMP)	73, 33, 65	86, −0.9, −2	66	1.0	1.3	1.4

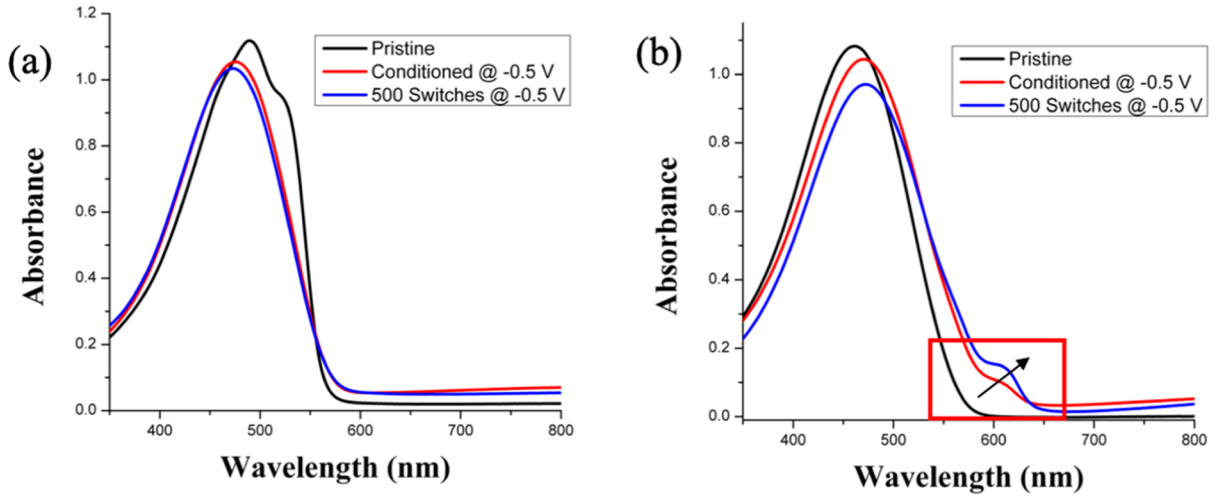

Figure 8. UV−vis absorbance spectra of (a) DAT-*co*-(ran-1,3-DMP) and (b) DAT-*co*-(reg-1,3-DMP) as pristine, electrochemically conditioned, and electrochemically cycled thin films.

the quantified difference in color DAT-*co*-(ran-1,3-DMP) after 500 electrochemical switching cycles is 1.5, which indicates that the minimal changes in the UV−vis absorbance spectrum do not lead to noticeable differences in color. Alternatively, due to the decrease in the $\pi-\pi^*$ transition of DAT-*co*-(reg-1,3-DMP) accompanied with the increased intensity of the transition ∼600 nm, the quantified color difference of DAT-*co*-(reg-1,3-DMP) is calculated as 9.0. Furthermore, the quantified color differences are supported with photography, where in Figure S10, DAT-*co*-(reg-1,3-DMP) evolves to a shade of brown, while DAT-*co*-(ran-1,3-DMP) maintains its orange hue with a slight decrease in saturation. The evolution of the absorbance profiles upon repeated electrochemical switching, and ultimately, changes in the film color, suggest that the polymer chain conformation that DAT-*co*-(reg-1,3-DMP) adopts in the solid state is less stable compared to DAT-*co*-(ran-1,3-DMP). The cause of this instability may be molecular weight effects or introduction of stereospecificity into the polymer backbone. At present, we are unable to identify the driving factor behind this observation, which further motivates the structural studies proposed previously in the manuscript.

The switching rate of the 1,3-DMP copolymers was studied by monitoring the change in transmittance (ΔT (%)) at the maximum absorbance wavelength as a function of time by applying square-wave potential steps (−0.5 to 0.6 V vs Ag/Ag^+ in 0.5 M $TBAPF_6$/PC) to polymer films spray-cast onto ITO electrodes for a range from 0.25 to 10 s. Details regarding the area and resistance of the electrodes are provided in the Supporting Information. As shown in Figure S11 and Table 3, at switching times above 2 s, both polymers exhibit ΔT (%) values from 66 to 70%. As the switching time is decreased to 0.25 s, the ΔT (%) values also decrease, as expected. This trend is indicative of both copolymers being rapid switching materials and is quantified by the time it takes both copolymers to reach 95% of a full contrast switch (t_{95}). As shown in Table 3, both copolymers exhibit bleaching times ∼1 s and coloration times ∼1.0−1.3 s. Furthermore, Table 3 shows that the standardized switching time (τ), which is obtained by fitting the data in Figure S11 to an exponential expression that correlates optical contrast with the time needed to obtain it,[89] is similar regardless of stereospecificity. The similar ΔT (%), t_{95}, and τ values for these DAT-based copolymers are an indication that, although optical and color properties are influenced by stereospecificity, properties such as contrast and switching times are minimally affected.

Regioisomer and 2,2-Functionality Effects. While electrochromic properties, such as contrast and switching times, were minimally influenced by stereospecificity, the observed differences of optical properties, color, and color stability motivated us to further probe isomeric effects on additional ECPs. Subsequently, a family of ProDOT copolymers 2,2-functionalized with methyl (DMP), ethyl (DEP), and isobutyl (D*i*BP) groups were synthesized as a means to probe compositional isomer effects. First, as shown in Figure S12 and tabulated in Table 4, all three DAT-*co*-(2,2-ProDOT)s exhibit broad featureless absorbance profiles in toluene solutions with λ_{max} values between 419 and 426 nm. Next, films were spray-cast from 5 mg/mL toluene solutions and UV−vis absorbance spectra were measured. As shown in Figure 9a, as pristine films, these copolymers exhibit broad, featureless absorbance profiles with λ_{max} values from 486 to

Table 4. Optical and Redox Properties of 2,2-Substituted ProDOT Copolymers

polymer	λ_{max}^{soln} (nm)	λ_{max}^{film} (nm)	λ_{onset}^{film} (nm)	E_{onset}^{ox} (V)
DAT-*co*-DMP	419	486	613	−0.10
DAT-*co*-DEP	419	497	616	−0.10
DAT-*co*-DiBP	426	494	613	0.21

https://dx.doi.org/10.1021/acs.macromol.0c02719
Macromolecules 2021, 54, 1677−1692

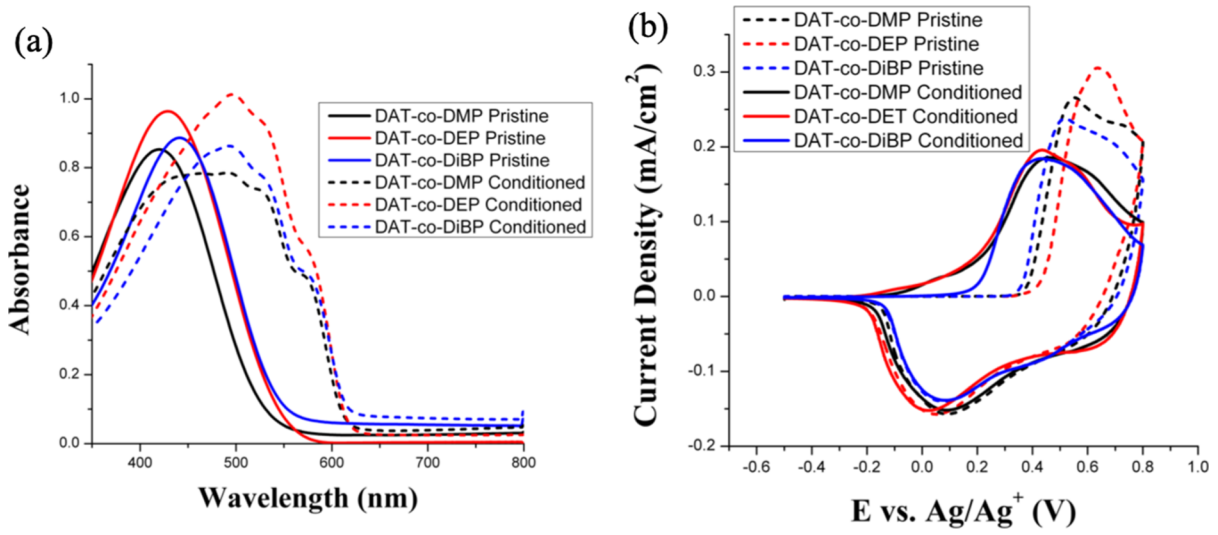

Figure 9. (a) UV−vis absorbance spectra (350−800 nm) and (b) cyclic voltammograms of pristine and electrochemically conditioned films of 2,2-functionalized DAT-*co*-ProDOT copolymers. Electrochemical conditioning protocols consist of performing 10 CV cycles across a voltage window of −0.5 to 0.8 V (vs Ag/Ag^+ reference electrode) in a 0.5 M $TBAPF_6$/PC electrolyte solution using a scan rate of 100 mV/s.

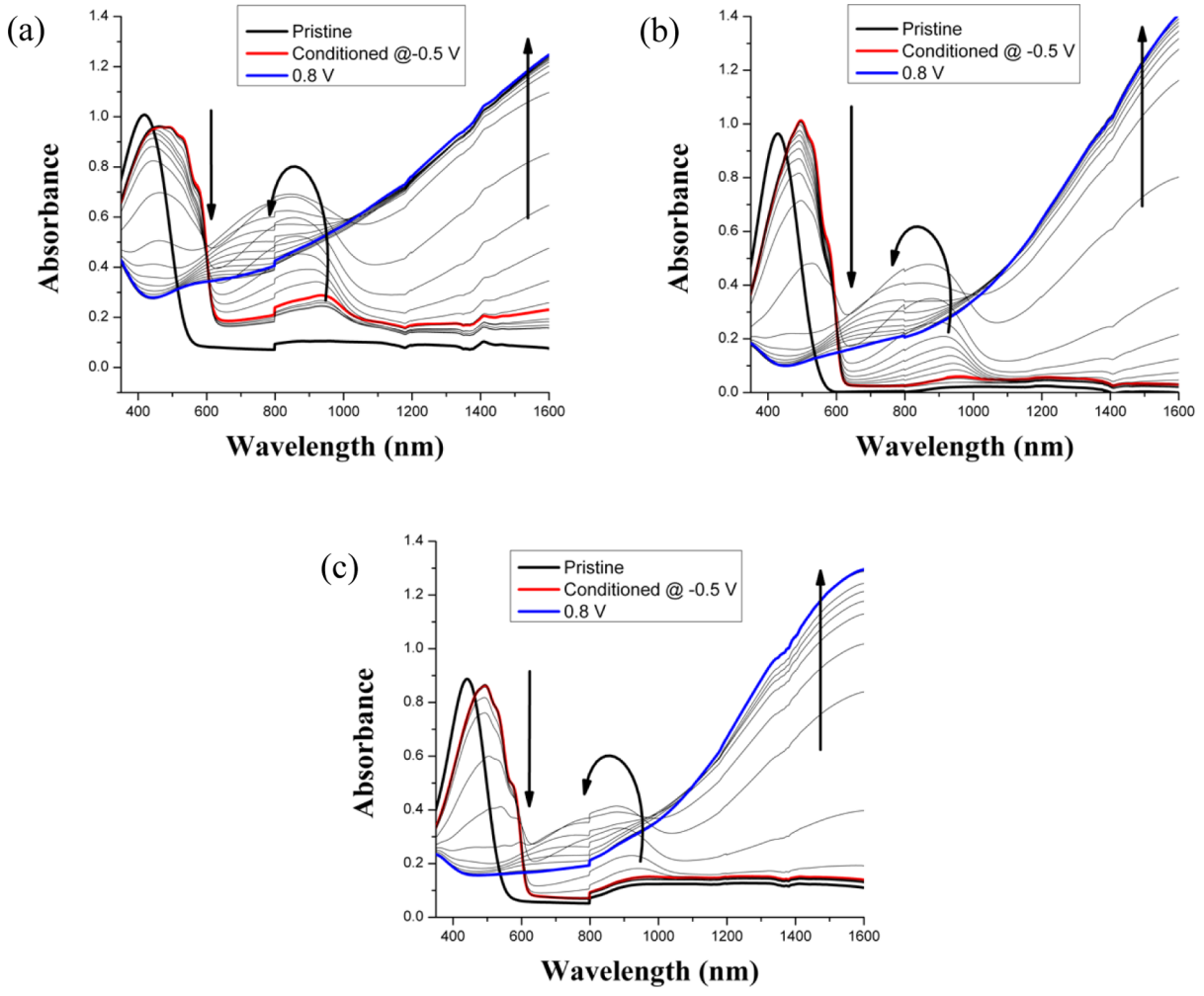

Figure 10. Absorbance spectra as a function of potential of (a) DAT-*co*-DMP, (b) DAT-*co*-DEP, and (c) DAT-*co*-D*i*BP spray-cast from 5 mg/mL toluene solutions by applying 50 mV potential intervals from −0.5 to 0.8 V in 0.5 M $TBAPF_6$/PC electrolyte.

497 nm. Upon electrochemical conditioning with 10 CV cycles from −0.5 to 0.8 V versus Ag/Ag^+ in 0.5 M $TBAPF_6$, all three 2,2-ProDOT copolymers exhibit distinct red-shifts and broader absorbance spectra that include fine-structure absorbance features ∼550 and ∼600 nm when compared to 1,3-ProDOTs copolymers in Figure 4a. Notably, these copolymers maintain

https://dx.doi.org/10.1021/acs.macromol.0c02719
Macromolecules 2021, 54, 1677−1692

absorbance in the high-energy region of the visible spectrum analogous to 1,3-ProDOTs but exhibit the fine-structure features of unsubstituted DAT-*co*-ProDOT.[41] The observed fine-structure features suggest the 2,2-ProDOTs possess a higher degree of ordering in the electrochemically conditioned films compared to 1,3-ProDOTs and facilitate improved cofacial π-stacking and interchain absorbance contributions commonly observed for polythiophenes.[90]

The electrochemical properties of the 2,2-ProDOT copolymers are illustrated in Figure 9b and reported in Table 4. As pristine films, all three polymers display onsets of oxidation between ∼0.3 and 0.4 V, as well as similar current densities and CV shapes. After electrochemical conditioning, as depicted by the solid lines, each CV trace is nearly identical with respect to shape and current density (∼0.2 mA/cm^2) when films are processed to a transmittance (%T) ≈ 10−15%. These similarities indicate that, regardless of the choice of functionality within this family, the underlying morphologies do not affect the accessible redox active sites in the polymer film and ultimately, the redox capacity of the films. The only variation observed was in the case of DAT-*co*-D*i*BP, which has a higher onset of oxidation (∼0.2 V vs Ag/Ag$^+$) after conditioning compared to an onset of oxidation ∼ −0.1 V versus Ag/Ag$^+$ for DAT-*co*-DMP and DAT-*co*-DEP. The differences in onsets of oxidation is an unusual observation considering the onset of absorbance and general profiles of the absorbance spectra are nearly identical. Combined, these results suggest the branched *iso*-butyl groups inhibit efficient electron transfer at the polymer/electrode interface, which has been demonstrated to be side chain-dependent in dioxythiophene copolymers.[91]

The changes in absorbance as a function of electrochemical potential from −0.5 to 0.8 V versus Ag/Ag$^+$ were evaluated for the DAT-*co*-(2,2-ProDOT) copolymers spray-cast onto ITO electrodes from 5 mg/mL toluene solutions. As shown in Figure 10, the absorbance of neutral DAT-*co*-DMP and DAT-*co*-DEP begins to decrease ∼−0.1 V versus Ag/Ag$^+$, while DAT-*co*-D*i*BP begins to decrease at ∼0.2 V, correlating with their oxidation onset. As the applied voltage is increased in 50 mV steps, the absorbance shoulders ∼550 and ∼600 nm decrease in intensity and the formation of polarons ∼900 nm is observed. With continued increase in the electrochemical potential, all three polymer films demonstrate a complete depletion of absorbance in the visible spectrum and form bipolaronic species >1400 nm. The diminished absorbance indicates that all three polymers transition from a colored neutral state to a highly transmissive film when oxidized above 0.6 V versus Ag/Ag$^+$.

Turning to colorimetry results, as shown in Figure 11, pristine films of all of the polymers are a vibrant yellow color. Upon electrochemical conditioning, the films undergo a distinct color change, yielding similar hues of red electrochromes. This observed color change agrees with the drastic "break-in" effect observed in the UV−vis spectra depicted in Figure 9. As observed in Figure 11 and tabulated in Table 5, the conditioned 2,2-ProDOT copolymers exhibit similar a* values (42−53), where variations among these values are attributed to differences in the transmittance of the films. Analogously, b* and L* values also are similar, which indicates the minimal changes to the 2,2-functionality does not have a significant influence on the color properties. The ability to access these red hues is attributed to the breadth of the absorbance profiles spanning >200 nm (400−625 nm) across

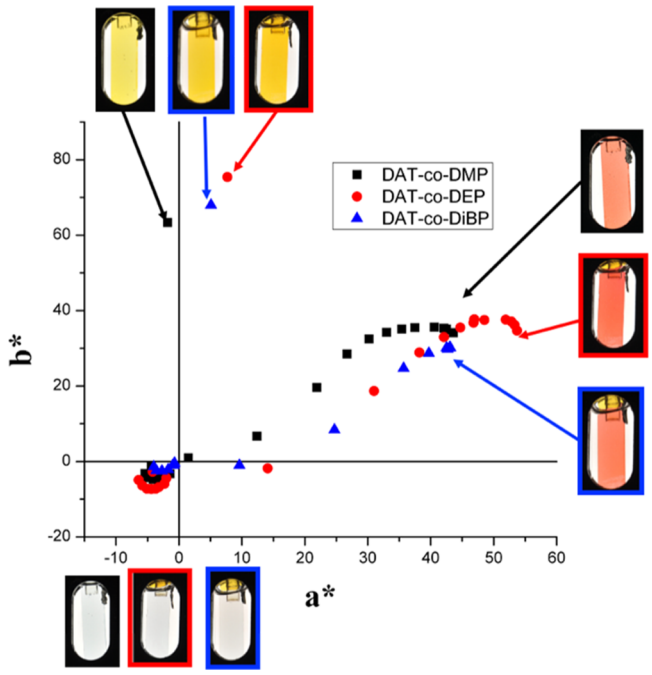

Figure 11. Color coordinates and photographs of DAT-*co*-DMP, DAT-*co*-DEP, and DAT-*co*-D*i*BP films spray-cast from toluene obtained as a function of potential.

the visible spectrum. As shown in Figure 11, each 2,2-ProDOT copolymer transitions from a colored film in the neutral state to a highly transmissive film with increasing oxidation potential with a* and b* values decreasing to values less than 5, respectively, as well as L* values >85. Combined, and as shown by the photographs, these values indicate the polymers reach a highly transmissive, color-neutral oxidized state.

As previously alluded to, and visualized in the photographs of Figure 11, differences in the transmittance of these films influence how saturated the red color is perceived by the human eye. These subtle changes led us to quantify these effects using colorimetry and photography. First, as shown in Figure 12a, DAT-*co*-ProDOT appears pink when spray-cast to a transmittance of ∼15% with a* and b* values ∼60 and ∼15, respectively. As the transmittance of the films is decreased, ultimately to ∼2% for the photograph highlighted in the blue box, a highly saturated red film is obtained with a* and b* values ∼80 and ∼50, respectively. Regardless of the transmittance, DAT-*co*-ProDOT transitions from a colored film in the neutral state to a highly transmissive film when oxidized, while maintaining the ability to rapidly switch between the colored and transmissive state (Figure S13). Furthermore, as shown in Figure 12b, when DAT-*co*-D*i*BP is spray cast to a transmittance ∼3%, a* and b* values ∼65 and ∼60 are measured, respectively, and photography reveals a highly saturated red film. To further analyze the quantification of these red electrochromes, color coordinates of "thick" films of DAT-*co*-ProDOT and DAT-*co*-D*i*BP are plotted alongside Munsell color points in Figure 12b, where the wedge between 2.5R and 7.5R is defined as an acceptable "red" region by the Munsell Color System,[40] and 5R is considered "pure red". The color coordinates for DAT-*co*-ProDOT fall between the 5R and 7.5R lines, and the accompanying photography validates the defined red region. Alternatively, color coordinates of DAT-*co*-D*i*BP fall slightly outside of the red wedge, which is attributed to the increased absorbance from 380 to ∼450 nm

https://dx.doi.org/10.1021/acs.macromol.0c02719
Macromolecules 2021, 54, 1677−1692

Table 5. Electrochromic Properties of 2,2-Substitued ProDOT Copolymers as Electrochemically Conditioned Films

	$L^*a^*b^*$					
polymer	neutral state	oxidized state	ΔT (%)	bleaching t_{95} (s)	coloration t_{95} (s)	τ (s)
DAT-*co*-DMP	67, 43, 34	87, −1, −3	64	1.6	1.1	0.8
DAT-*co*-DEP	62, 53, 34	88, −2, −4	67	1.3	1.3	0.6
DAT-*co*-D*i*BP	65, 42, 29	86, −0.7, −0.4	63	1.3	1.0	0.4

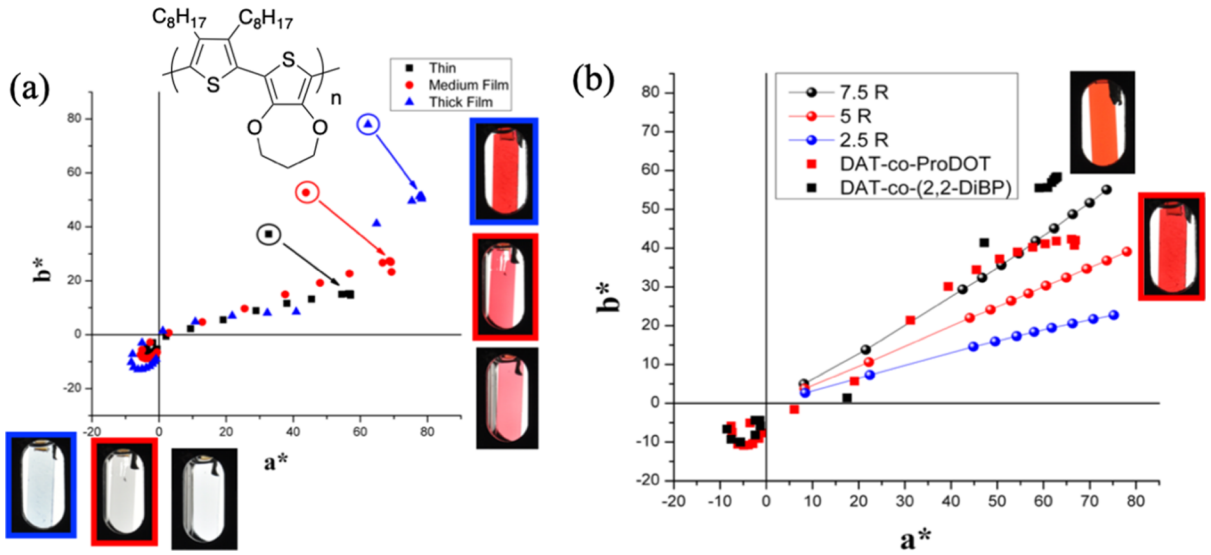

Figure 12. Comparison of color coordinates and photographs for "thick" films of DAT-*co*-ProDOT and DAT-*co*-(2,2-D*i*BP).

measured for the 2,2-ProDOT copolymers compared to DAT-*co*-ProDOT. The increased absorbance between 380 and 450 nm translates to DAT-*co*-D*i*BP possessing a slight orange hue compared to DAT-*co*-ProDOT.

While 2,2-functionality has yielded only minimal differences in the fundamental optical, electrochemical, and color properties of DAT-*co*-(2,2-ProDOTs), significant changes reveal themselves after repeated electrochemical cycling (500 redox cycles) between −0.5 and 0.6 V versus Ag/Ag^+ in 0.5 M $TBAPF_6$/PC electrolyte under an Ar atmosphere. While each polymer displays electrochemical stability over the course of the experiments (Figure 13a), the optical, and ultimately color properties, show a strong dependence on 2,2-substitution. First, Figure 13b shows DAT-*co*-DMP exhibits a distinct red-shift in the absorbance pattern as well as further evolution of vibronic fine-structure features in the UV−vis absorbance spectrum. When the 2,2-substituent is changed to ethyl groups (Figure 13c), changes in the absorbance spectrum are reduced, but distinct differences are still observed. In the case of DAT-*co*-D*i*BP, the absorbance spectrum is essentially unchanged after 500 electrochemical redox cycles (Figure 13d). These results suggest that DAT-*co*-D*i*BP is in a more stable conformation in the solid state after initial electrochemical conditioning protocols compared to DAT-*co*-DMP and DAT-*co*-DEP and maintains this stability after repeated electrochemical cycles. The changes in the absorbance spectra are further quantified by calculating the quantified color change (ΔE^*_{ab}) between electrochemically conditioned films and films that have been switched with 500 redox cycles. The ΔE^*_{ab} calculated for the DAT-*co*-(2,2-ProDOT) copolymers are tabulated in Table S6 and follow the trend of *decreasing* ΔE^*_{ab} with *increasing* substituent bulk at the 2,2-position of the propylene bridge. The changes measured in the UV−vis results in DAT-*co*-DMP and DAT-*co*-DEP having a visibly different color, while DAT-*co*-D*i*BP demonstrates superior color stability (ΔE^*_{ab} = 1.8) not detectable by the human eye after extensive electrochemical switching. Ultimately, these experiments reveal how subtle structural changes to the 2,2-position of ProDOT comonomers influence the long-term color switching properties of high-gap electrochromic copolymers.

The switching rate of the 2,2-functionalized copolymers was studied by monitoring the change in transmittance (ΔT (%)) at the maximum absorbance wavelength as a function of time by applying square-wave potential steps (−0.5 to 0.6 V vs Ag/Ag^+ in 0.5 M $TBAPF_6$/PC) to polymer films spray-cast onto ITO electrodes for a range from 0.25 to 10 s. As shown in Figure S14 and Table 5, at switching times above 2 s, the 2,2-functionalized copolymers exhibit ΔT (%) values ∼65%. Analogous to 1,3-functionalized copolymers, the 2,2-functionalized copolymers are rapidly switching materials and is confirmed by the time it takes all three copolymers to reach 95% of a full contrast switch (t_{95}). Specifically, all three copolymers exhibit bleaching and coloration times ∼1 s (see Table 5). Notably, as the substituent bulk is *increased* at the 2,2-position of the propylene bridge, the standardized switching time, τ, slightly *decreases*. This trend is in agreement with previous studies demonstrating that increasing the size of the solubilizing side chain at the 2,2-position of the propylene bridge improves the switching kinetics of ProDOT polymers.[67] The similar ΔT (%) and t_{95} values, in addition to modest differences of τ values for these DAT-based copolymers, indicates that subtle differences of the 2,2-functionality minimally influences properties such as contrast and switching times.

https://dx.doi.org/10.1021/acs.macromol.0c02719
Macromolecules 2021, 54, 1677−1692

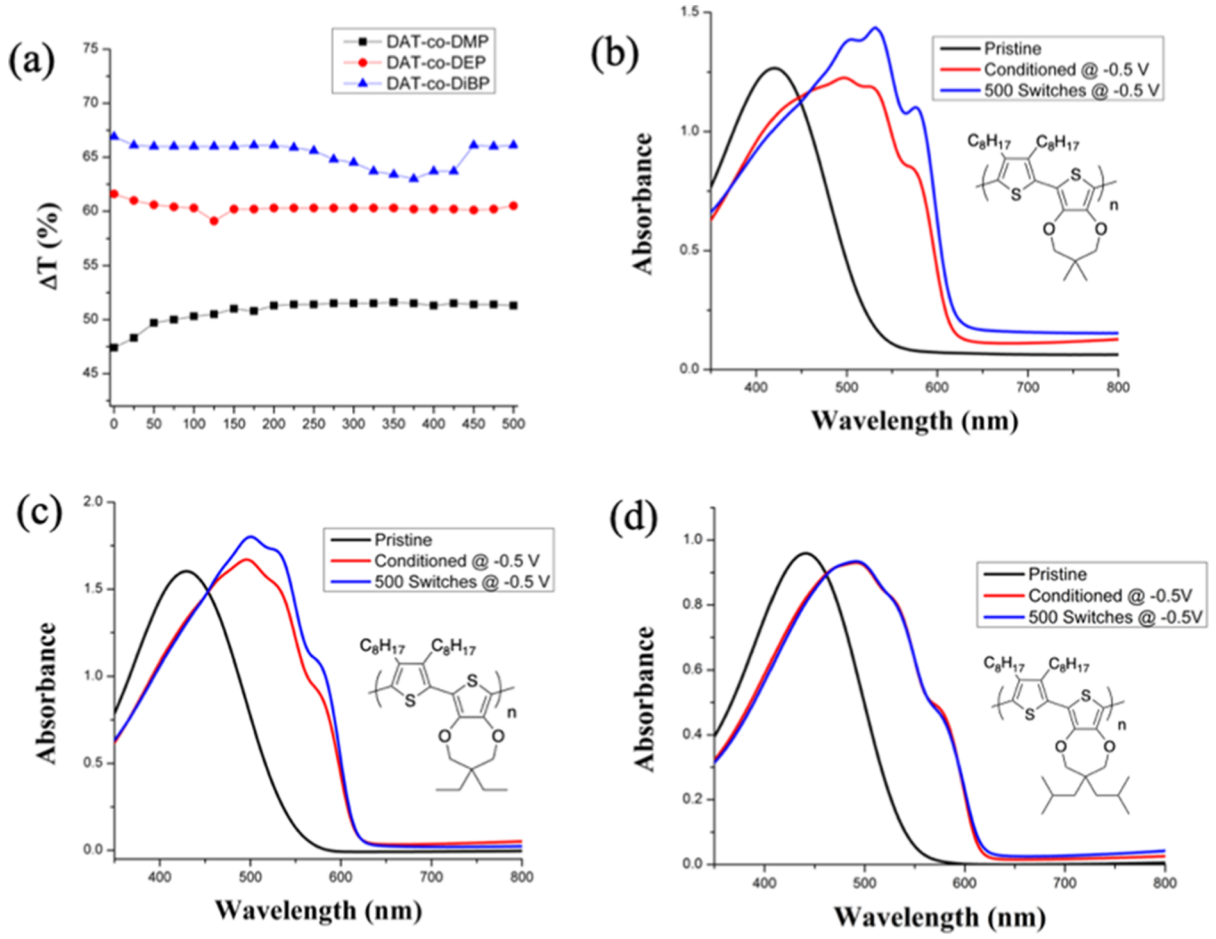

Figure 13. (a) Contrast (ΔT (%)) versus the number of redox switching cycles of DAT-*co*-(2,2-ProDOT) copolymers while applying square-wave potentials between −0.5 and 0.6 V vs Ag/Ag^+ in a 0.5 M $TBAPF_6$/PC electrolyte solution. UV−vis absorbance spectra of (b) DAT-*co*-DMP, (c) DAT-*co*-DEP, and (d) DAT-*co*-D*i*BP as pristine, electrochemically conditioned, and electrochemically cycled thin films.

CONCLUSIONS

Understanding how subtle structural features influence optical and electrochemical properties of redox-active conjugated ECPs is essential for establishing design motifs to fine-tune application-inspired properties, such as color control in electrochromism. This study expands this understanding to encompass the influence of compositional isomers on color control of high-gap ECPs. TD-DFT calculations lend credence to the hypothesis that subtle changes in stereospecificity and substitution pattern across the propylene bridge of ProDOT comonomers yield distinct shifts in calculated absorbance spectra and color. Guided by computation, stereo- and regiospecific copolymers were synthesized via direct arylation polymerization to yield a family of electrochromic copolymers in the orange/red color space that transition from deeply colored films in the neutral state to highly transmissive films with an applied electrochemical potential. Notably, the entire family of DAT-based copolymers exhibit excellent contrast and kinetic switching times (ΔT (%) ≈ 65% and t_{95} ≈ 1 s, respectively), regardless of substitution pattern within the alternating copolymers. By elucidating these structural influences, this study will be used to guide the future design of conjugated polymers that are useful in redox-active applications, especially fine-tuning color control of ECPs.

ASSOCIATED CONTENT

Supporting Information

The Supporting Information is available free of charge at https://pubs.acs.org/doi/10.1021/acs.macromol.0c02719.

Materials and methods, computational details, synthetic procedures, ^1H and ^{13}C of monomers and polymers, SEC, and chronoabsorptiometry data (PDF)

AUTHOR INFORMATION

Corresponding Author

John R. Reynolds − *School of Chemistry and Biochemistry, School of Materials Science and Engineering, Center for Organic Photonics and Electronics, Georgia Tech Polymer Network, Georgia Institute of Technology, Atlanta, Georgia 30332, United States;* orcid.org/0000-0002-7417-4869; Email: reynolds@chemistry.gatech.edu

Authors

Graham S. Collier − *School of Chemistry and Biochemistry, School of Materials Science and Engineering, Center for Organic Photonics and Electronics, Georgia Tech Polymer Network, Georgia Institute of Technology, Atlanta, Georgia 30332, United States; Department of Chemistry and Biochemistry, Kennesaw State University, Kennesaw, Georgia 30144, United States;* orcid.org/0000-0002-9650-8110

Riley Wilkins − *Department of Chemistry and Biochemistry, University of North Georgia, Dahlonega, Georgia 30597, United States*

Aimée L. Tomlinson − *Department of Chemistry and Biochemistry, University of North Georgia, Dahlonega, Georgia 30597, United States*

Complete contact information is available at: https://pubs.acs.org/10.1021/acs.macromol.0c02719

Notes

The authors declare the following competing financial interest(s): Electrochromic polymer technology developed at the Georgia Institute of Technology has been licensed to NXN Licensing. GSC and JRR serve as consultants to NXN Licensing.

■ ACKNOWLEDGMENTS

Funding from the Air Force Office of Scientific Research (Award #: FA9550-18-1-0184) for this work is acknowledged. Dr. Zach Siebers and Brandon DiTullio are acknowledged for DSC data acquisition and helpful discussion.

■ REFERENCES

(1) Ibanez, J. G.; Rincón, M. E.; Gutierrez-Granados, S.; Chahma, M. h.; Jaramillo-Quintero, O. A.; Frontana-Uribe, B. A. Conducting Polymers in the Fields of Energy, Environmental Remediation, and Chemical−Chiral Sensors. *Chem. Rev.* **2018**, *118*, 4731−4816.

(2) Bryan, A. M.; Santino, L. M.; Lu, Y.; Acharya, S.; D'Arcy, J. M. Conducting Polymers for Pseudocapacitive Energy Storage. *Chem. Mater.* **2016**, *28*, 5989−5998.

(3) Kaloni, T. P.; Giesbrecht, P. K.; Schreckenbach, G.; Freund, M. S. Polythiophene: From Fundamental Perspectives to Applications. *Chem. Mater.* **2017**, *29*, 10248−10283.

(4) Beaujuge, P. M.; Reynolds, J. R. Color Control in π-Conjugated Organic Polymers for Use in Electrochromic Devices. *Chem. Rev.* **2010**, *110*, 268−320.

(5) Li, X.; Perera, K.; He, J.; Gumyusenge, A.; Mei, J. Solution-Processable Electrochromic Materials and Devices: Roadblocks and Strategies Towards Large-Scale Applications. *J. Mater. Chem. C* **2019**, *7*, 12761−12789.

(6) Fidanovski, K.; Mawad, D. Conjugated Polymers in Bioelectronics: Addressing the Interface Challenge. *Adv. Healthcare Mater.* **2019**, *8*, 1900053.

(7) Österholm, A. M.; Shen, D. E.; Reynolds, J. R. Electrochromism in Conjugated Polymer-Strategies for Complete and Straightfoward Color Control. In *Handbook of Conducting Polymers*, 4th ed.; Reynolds, J., Thompson, B., Skothelm, T., Eds.; CRC Press: Boca Routon, 2019; Vol. 4.

(8) Lo, C. K.; Shen, D. E.; Reynolds, J. R. Fine-Tuning the Color Hue of π-Conjugated Black-to-Clear Electrochromic Random Copolymers. *Macromolecules* **2019**, *52*, 6773−6779.

(9) Öktem, G.; Balan, A.; Baran, D.; Toppare, L. Donor−Acceptor Type Random Copolymers for Full Visible Light Absorption. *Chem. Commun.* **2011**, *47*, 3933−3935.

(10) Neo, W. T.; Cho, C. M.; Shi, Z.; Chua, S.-J.; Xu, J. Modulating High-Energy Visible Light Absorption to Attain Neutral-State Black Electrochromic Polymers. *J. Mater. Chem. C* **2016**, *4*, 28−32.

(11) Chen, C.; Yan, Q. Achieving Excellent Colorimetric Properties of Low-Cost Black to Transmissive Switching Electrochromic Polymers by Incorporating of Spacing Units into Copolymers of 3,4-Propylenedioxythiophene and Benzothiadiazole. *Dyes Pigm.* **2020**, *178*, 108378.

(12) Bini, K.; Murto, P.; Elmas, S.; Andersson, M. R.; Wang, E. Broad Spectrum Absorption and Low-Voltage Electrochromic Operation from Indacenodithieno[3,2-b]thiophene-Based Copolymers. *Polym. Chem.* **2019**, *10*, 2004−2014.

(13) Li, W.; Ning, J.; Yin, Y.; Xing, X.; Qi, M.; Li, T.; Cao, J.; He, Y.; Perepichka, I. F.; Meng, H. Thieno[3,2-b]thiophene-Based Conjugated Copolymers for Solution-Processable Neutral Black Electrochromism. *Polym. Chem.* **2018**, *9*, 5608−5616.

(14) Christiansen, D. T.; Ohtani, S.; Chujo, Y.; Tomlinson, A. L.; Reynolds, J. R. All Donor Electrochromic Polymers Tunable across the Visible Spectrum via Random Copolymerization. *Chem. Mater.* **2019**, *31*, 6841−6849.

(15) Österholm, A. M.; Shen, D. E.; Kerszulis, J. A.; Bulloch, R. H.; Kuepfert, M.; Dyer, A. L.; Reynolds, J. R. Four Shades of Brown: Tuning of Electrochromic Polymer Blends Toward High-Contrast Eyewear. *ACS Appl. Mater. Interfaces* **2015**, *7*, 1413−1421.

(16) Savagian, L. R.; Österholm, A. M.; Shen, D. E.; Christiansen, D. T.; Kuepfert, M.; Reynolds, J. R. Conjugated Polymer Blends for High Contrast Black-to-Transmissive Electrochromism. *Adv. Opt. Mater.* **2018**, *6*, 1800594.

(17) Sassi, M.; Salamone, M. M.; Ruffo, R.; Patriarca, G. E.; Mari, C. M.; Pagani, G. A.; Posset, U.; Beverina, L. State-of-the-Art Neutral Tint Multichromophoric Polymers for High-Contrast See-Through Electrochromic Devices. *Adv. Funct. Mater.* **2016**, *26*, 5240−5246.

(18) Lee, K.-R.; Sotzing, G. A. Color Tuning of Black for Electrochromic Polymers Using Precursor Blends. *Chem. Commun.* **2013**, *49*, 5192−5194.

(19) Xu, Z.; Wang, W.; Wu, J.; Mi, S.; Zheng, J.; Xu, C. Black-to-Transmissive Electrochromic Switching Polymer Films via Solution Co-Processing. *New J. Chem.* **2016**, *40*, 5231−5237.

(20) Li, M.; Yassin, O. A.; Baczkowski, M. L.; Zhang, X.; Daniels, R.; Deshmukh, A. A.; Zhu, Y.; Otley, M. T.; Sotzing, G. A. Colorless to Black Electrochromic Devices using Subtractive Color Mixing of Two Electrochromes: A Conjugated Polymer with a Small Organic Molecule. *Org. Electron.* **2020**, *84*, 105748.

(21) Yu, X.; Chang, M.; Chen, W.; Liang, D.; Lu, X.; Zhou, G. Colorless-to-Black Electrochromism from Binary Electrochromes toward Multifunctional Displays. *ACS Appl. Mater. Interfaces* **2020**, *12*, 39505−39514.

(22) Yen, H.-J.; Liou, G.-S. Solution-Processable Triarylamine-Based Electroactive High Performance Polymers for Anodically Electrochromic Applications. *Polym. Chem.* **2012**, *3*, 255−264.

(23) Beaupré, S.; Dumas, J.; Leclerc, M. Toward the Development of New Textile/Plastic Electrochromic Cells Using Triphenylamine-Based Copolymers. *Chem. Mater.* **2006**, *18*, 4011−4018.

(24) Jeong, J.; Kumar, R. S.; Naveen, M.; Son, Y.-A. Synthesis and Characterization of Triphenylamine-Based Polymers and Their Application Towards Solid-State Electrochromic Cells. *RSC Adv.* **2016**, *6*, 78984−78993.

(25) Chen, W.-H.; Wang, K.-L.; Hung, W.-Y.; Jiang, J.-C.; Liaw, D.-J.; Lee, K.-R.; Lai, J.-Y.; Chen, C.-L. Novel Triarylamine-Based Alternating Conjugated Polymer with High Hole Mobility: Synthesis, Electro-Optical, and Electronic Properties. *J. Polym. Sci., Part A: Polym. Chem.* **2010**, *48*, 4654−4667.

(26) Dey, T.; Invernale, M. A.; Ding, Y.; Buyukmumcu, Z.; Sotzing, G. A. Poly(3,4-propylenedioxythiophene)s as a Single Platform for Full Color Realization. *Macromolecules* **2011**, *44*, 2415−2417.

(27) Alamer, F. A.; Otley, M. T.; Ding, Y.; Sotzing, G. A. Solid-State High-Throughput Screening for Color Tuning of Electrochromic Polymers. *Adv. Mater.* **2013**, *25*, 6256−6260.

(28) Amb, C. M.; Kerszulis, J. A.; Thompson, E. J.; Dyer, A. L.; Reynolds, J. R. Propylenedioxythiophene (ProDOT)−Phenylene Copolymers Allow a Yellow-to-Transmissive Electrochrome. *Polym. Chem.* **2011**, *2*, 812−814.

(29) Kerszulis, J. A.; Amb, C. M.; Dyer, A. L.; Reynolds, J. R. Follow the Yellow Brick Road: Structural Optimization of Vibrant Yellow-to-Transmissive Electrochromic Conjugated Polymers. *Macromolecules* **2014**, *47*, 5462−5469.

(30) Cao, K.; Shen, D. E.; Österholm, A. M.; Kerszulis, J. A.; Reynolds, J. R. Tuning Color, Contrast, and Redox Stability in High Gap Cathodically Coloring Electrochromic Polymers. *Macromolecules* **2016**, *49*, 8498−8507.

(31) İçli-Özkut, M.; Öztaş, Z.; Algi, F.; Cihaner, A. A Neutral State Yellow to Navy Polymer Electrochrome with Pyrene Scaffold. *Org. Electron.* **2011**, *12*, 1505−1511.
(32) Oguzhan, E.; Bilgili, H.; Baycan Koyuncu, F.; Ozdemir, E.; Koyuncu, S. A New Processable Donor−Acceptor Polymer Displaying Neutral State Yellow Electrochromism. *Polymer* **2013**, *54*, 6283−6292.
(33) Dyer, A. L.; Craig, M. R.; Babiarz, J. E.; Kiyak, K.; Reynolds, J. R. Orange and Red to Transmissive Electrochromic Polymers Based on Electron-Rich Dioxythiophenes. *Macromolecules* **2010**, *43*, 4460−4467.
(34) Xu, Z.; Chen, X.; Mi, S.; Zheng, J.; Xu, C. Solution-Processable Electrochromic Red-to-Transmissive Polymers with Tunable Neutral State Colors, High Contrast and Enhanced Stability. *Org. Electron.* **2015**, *26*, 129−136.
(35) Chen, X.; Xu, Z.; Mi, S.; Zheng, J.; Xu, C. Spray-Processable Red-to-Transmissive Electrochromic Polymers Towards Fast Switching Time for Display Applications. *New J. Chem.* **2015**, *39*, 5389−5394.
(36) Garnier, F.; Tourillon, G.; Gazard, M.; Dubois, J. C. Organic Conducting Polymers Derived from Substituted Thiophenes as Electrochromic Material. *J. Electroanal. Chem. Interfacial Electrochem.* **1983**, *148*, 299−303.
(37) Hızalan, G.; Balan, A.; Baran, D.; Toppare, L. Spray Processable Ambipolar Benzotriazole Bearing Electrochromic Polymers with Multi-Colored and Transmissive States. *J. Mater. Chem.* **2011**, *21*, 1804−1809.
(38) Atakan, G.; Gunbas, G. A Novel Red to Transmissive Electrochromic Polymer Based on Phenanthrocarbazole. *RSC Adv.* **2016**, *6*, 25620−25623.
(39) Cho, C. M.; Ye, Q.; Neo, W. T.; Lin, T.; Song, J.; Lu, X.; Xu, J. Red-to-Black Electrochromism of 4,9-Dihydro-s-indaceno[1,2-b:5,6-b']dithiophene-Embedded Conjugated Polymers. *J. Mater. Sci.* **2015**, *50*, 5856−5864.
(40) Yin, Y.; Li, W.; Zeng, X.; Xu, P.; Murtaza, I.; Guo, Y.; Liu, Y.; Li, T.; Cao, J.; He, Y.; Meng, H. Design Strategy for Efficient Solution-Processable Red Electrochromic Polymers Based on Unconventional 3,6-Bis(dodecyloxy)thieno[3,2-b]thiophene Building Blocks. *Macromolecules* **2018**, *51*, 7853−7862.
(41) Christiansen, D. T.; Reynolds, J. R. A Fruitful Usage of a Dialkylthiophene Comonomer for Redox Stable Wide-Gap Cathodically Coloring Electrochromic Polymers. *Macromolecules* **2018**, *51*, 9250−9258.
(42) Kohn, P.; Huettner, S.; Komber, H.; Senkovskyy, V.; Tkachov, R.; Kiriy, A.; Friend, R. H.; Steiner, U.; Huck, W. T. S.; Sommer, J.-U.; Sommer, M. On the Role of Single Regiodefects and Polydispersity in Regioregular Poly(3-hexylthiophene): Defect Distribution, Synthesis of Defect-Free Chains, and a Simple Model for the Determination of Crystallinity. *J. Am. Chem. Soc.* **2012**, *134*, 4790−4805.
(43) Snyder, C. R.; Henry, J. S.; DeLongchamp, D. M. Effect of Regioregularity on the Semicrystalline Structure of Poly(3-hexylthiophene). *Macromolecules* **2011**, *44*, 7088−7091.
(44) Willot, P.; Steverlynck, J.; Moerman, D.; Leclère, P.; Lazzaroni, R.; Koeckelberghs, G. Poly(3-alkylthiophene) with Tuneable Regioregularity: Synthesis and Self-Assembling Properties. *Polym. Chem.* **2013**, *4*, 2662−2671.
(45) Jiang, X. M.; Österbacka, R.; Korovyanko, O.; An, C. P.; Horovitz, B.; Janssen, R. A. J.; Vardeny, Z. V. Spectroscopic Studies of Photoexcitations in Regioregular and Regiorandom Polythiophene Films. *Adv. Funct. Mater.* **2002**, *12*, 587−597.
(46) Sirringhaus, H.; Brown, P. J.; Friend, R. H.; Nielsen, M. M.; Bechgaard, K.; Langeveld-Voss, B. M. W.; Spiering, A. J. H.; Janssen, R. A. J.; Meijer, E. W.; Herwig, P.; de Leeuw, D. M. Two-Dimensional Charge Transport in Self-Organized, High-Mobility Conjugated Polymers. *Nature* **1999**, *401*, 685−688.
(47) Mauer, R.; Kastler, M.; Laquai, F. The Impact of Polymer Regioregularity on Charge Transport and Efficiency of P3HT:PCBM Photovoltaic Devices. *Adv. Funct. Mater.* **2010**, *20*, 2085−2092.
(48) Kim, J.-S.; Kim, J.-H.; Lee, W.; Yu, H.; Kim, H. J.; Song, I.; Shin, M.; Oh, J. H.; Jeong, U.; Kim, T.-S.; Kim, B. J. Tuning Mechanical and Optoelectrical Properties of Poly(3-hexylthiophene) through Systematic Regioregularity Control. *Macromolecules* **2015**, *48*, 4339−4346.
(49) Park, H.; Ma, B. S.; Kim, J.-S.; Kim, Y.; Kim, H. J.; Kim, D.; Yun, H.; Han, J.; Kim, F. S.; Kim, T.-S.; Kim, B. J. Regioregular-block-Regiorandom Poly(3-hexylthiophene) Copolymers for Mechanically Robust and High-Performance Thin-Film Transistors. *Macromolecules* **2019**, *52*, 7721−7730.
(50) Osaka, I.; McCullough, R. D. Regioregular and Regiosymmetric Polythiophenes. *Conjugated Polymer Synthesis: Methods and Reactions*; Wiley, 2010; pp 59−90.
(51) Gallazzi, M. C.; Castellani, L.; Marin, R. A.; Zerbi, G. Regiodefined Substituted Poly(2,5-thienylene)s. *J. Polym. Sci., Part A: Polym. Chem.* **1993**, *31*, 3339−3349.
(52) Ong, B. S.; Wu, Y.; Liu, P.; Gardner, S. High-Performance Semiconducting Polythiophenes for Organic Thin-Film Transistors. *J. Am. Chem. Soc.* **2004**, *126*, 3378−3379.
(53) Kline, R. J.; DeLongchamp, D. M.; Fischer, D. A.; Lin, E. K.; Richter, L. J.; Chabinyc, M. L.; Toney, M. F.; Heeney, M.; McCulloch, I. Critical Role of Side-Chain Attachment Density on the Order and Device Performance of Polythiophenes. *Macromolecules* **2007**, *40*, 7960−7965.
(54) McCulloch, I.; Heeney, M.; Bailey, C.; Genevicius, K.; MacDonald, I.; Shkunov, M.; Sparrowe, D.; Tierney, S.; Wagner, R.; Zhang, W.; Chabinyc, M. L.; Kline, R. J.; McGehee, M. D.; Toney, M. F. Liquid-Crystalline Semiconducting Polymers with High Charge-Carrier Mobility. *Nat. Mater.* **2006**, *5*, 328−333.
(55) Osaka, I.; Abe, T.; Shinamura, S.; Takimiya, K. Impact of Isomeric Structures on Transistor Performances in Naphthodithiophene Semiconducting Polymers. *J. Am. Chem. Soc.* **2011**, *133*, 6852−6860.
(56) Monika; Verma, A.; Tiwari, M. K.; Show, B.; Saha, S. Modulation of Weak Interactions in Structural Isomers: Positional Isomeric Effects on Crystal Packing and Physical Properties and Solid-State Thin-Film Fabrication. *ACS Omega* **2020**, *5*, 448−459.
(57) Wang, J.; Zhang, J.; Xiao, Y.; Xiao, T.; Zhu, R.; Yan, C.; Fu, Y.; Lu, G.; Lu, X.; Marder, S. R.; Zhan, X. Effect of Isomerization on High-Performance Nonfullerene Electron Acceptors. *J. Am. Chem. Soc.* **2018**, *140*, 9140−9147.
(58) Fronk, S. L.; Wang, M.; Ford, M.; Coughlin, J.; Mai, C.-K.; Bazan, G. C. Effect of Chiral 2-Ethylhexyl Side Chains on Chiroptical Properties of the Narrow Bandgap Conjugated Polymers PCPDTBT and PCDTPT. *Chem. Sci.* **2016**, *7*, 5313−5321.
(59) Ikai, T.; Yoshida, T.; Awata, S.; Wada, Y.; Maeda, K.; Mizuno, M.; Swager, T. M. Circularly Polarized Luminescent Triptycene-Based Polymers. *ACS Macro Lett.* **2018**, *7*, 364−369.
(60) Watanabe, K.; Akagi, K. Helically Assembled π-Conjugated Polymers with Circularly Polarized Luminescence. *Sci. Technol. Adv. Mater.* **2014**, *15*, 044203.
(61) Pop, F.; Zigon, N.; Avarvari, N. Main-Group-Based Electro- and Photoactive Chiral Materials. *Chem. Rev.* **2019**, *119*, 8435−8478.
(62) Caras-Quintero, D.; Bäuerle, P. Synthesis of the First Enantiomerically Pure and Chiral, Disubstituted 3,4-Ethylenedioxythiophenes (EDOTs) and Corresponding Stereo- and Regioregular PEDOTs. *Chem. Commun.* **2004**, 926−927.
(63) Caras-Quintero, D.; Bäuerle, P. Efficient Synthesis of 3,4-Ethylenedioxythiophenes (EDOT) by Mitsunobu Reaction. *Chem. Commun.* **2002**, 2690−2691.
(64) Amsallem, D.; Bedi, A.; Tassinari, F.; Gidron, O. Relation between Morphology and Chiroptical Properties in Chiral Conducting Polymer Films: A Case Study in Chiral PEDOT. *Macromolecules* **2020**, *53*, 9521−9528.
(65) Grenier, C. R. G.; Pisula, W.; Joncheray, T. J.; Müllen, K.; Reynolds, J. R. Regiosymmetric Poly(dialkylphenylenedioxythiophene)s: Electron-Rich, Stackable π-Conjugated Nanoribbons. *Angew. Chem., Int. Ed.* **2007**, *46*, 714−717.

https://dx.doi.org/10.1021/acs.macromol.0c02719
Macromolecules 2021, 54, 1677−1692

(66) Welsh, D. M.; Kloeppner, L. J.; Madrigal, L.; Pinto, M. R.; Thompson, B. C.; Schanze, K. S.; Abboud, K. A.; Powell, D.; Reynolds, J. R. Regiosymmetric Dibutyl-Substituted Poly(3,4-propylenedioxythiophene)s as Highly Electron-Rich Electroactive and Luminescent Polymers. *Macromolecules* **2002**, *35*, 6517−6525.
(67) Reeves, B. D.; Grenier, C. R. G.; Argun, A. A.; Cirpan, A.; McCarley, T. D.; Reynolds, J. R. Spray Coatable Electrochromic Dioxythiophene Polymers with High Coloration Efficiencies. *Macromolecules* **2004**, *37*, 7559−7569.
(68) Grenier, C. R. G.; George, S. J.; Joncheray, T. J.; Meijer, E. W.; Reynolds, J. R. Chiral Ethylhexyl Substituents for Optically Active Aggregates of π-Conjugated Polymers. *J. Am. Chem. Soc.* **2007**, *129*, 10694−10699.
(69) Yang, X.; Seo, S.; Park, C.; Kim, E. Electrical Chiral Assembly Switching of Soluble Conjugated Polymers from Propylenedioxythiophene-Phenylene Copolymers. *Macromolecules* **2014**, *47*, 7043−7051.
(70) Wheeler, D. L.; Rainwater, L. E.; Green, A. R.; Tomlinson, A. L. Modeling Electrochromic Poly-Dioxythiophene-Containing Materials through TDDFT. *Phys. Chem. Chem. Phys.* **2017**, *19*, 20251−20258.
(71) Welsh, D. M.; Kumar, A.; Meijer, E. W.; Reynolds, J. R. Enhanced Contrast Ratios and Rapid Switching in Electrochromics Based on Poly(3,4-propylenedioxythiophene) Derivatives. *Adv. Mater.* **1999**, *11*, 1379−1382.
(72) Estrada, L. A.; Deininger, J. J.; Kamenov, G. D.; Reynolds, J. R. Direct (Hetero)arylation Polymerization: An Effective Route to 3,4-Propylenedioxythiophene-Based Polymers with Low Residual Metal Content. *ACS Macro Lett.* **2013**, *2*, 869−873.
(73) Pouliot, J.-R.; Grenier, F.; Blaskovits, J. T.; Beaupré, S.; Leclerc, M. Direct (Hetero)arylation Polymerization: Simplicity for Conjugated Polymer Synthesis. *Chem. Rev.* **2016**, *116*, 14225−14274.
(74) Gobalasingham, N. S.; Thompson, B. C. Direct Arylation Polymerization: A Guide to Optimal Conditions for Effective Conjugated Polymers. *Prog. Polym. Sci.* **2018**, *83*, 135−201.
(75) Collier, G. S.; Reynolds, J. R. Exploring the Utility of Buchwald Ligands for C−H Oxidative Direct Arylation Polymerizations. *ACS Macro Lett.* **2019**, *8*, 931−936.
(76) Lo, C. K.; Gautam, B. R.; Selter, P.; Zheng, Z.; Oosterhout, S. D.; Constantinou, I.; Knitsch, R.; Wolfe, R. M. W.; Yi, X.; Brédas, J.-L.; So, F.; Toney, M. F.; Coropceanu, V.; Hansen, M. R.; Gundogdu, K.; Reynolds, J. R. Every Atom Counts: Elucidating the Fundamental Impact of Structural Change in Conjugated Polymers for Organic Photovoltaics. *Chem. Mater.* **2018**, *30*, 2995−3009.
(77) Kaake, L.; Dang, X.-D.; Leong, W. L.; Zhang, Y.; Heeger, A.; Nguyen, T.-Q. Effects of Impurities on Operational Mechanism of Organic Bulk Heterojunction Solar Cells. *Adv. Mater.* **2013**, *25*, 1706−1712.
(78) Diemer, P. J.; Hayes, J.; Welchman, E.; Hallani, R.; Pookpanratana, S. J.; Hacker, C. A.; Richter, C. A.; Anthony, J. E.; Thonhauser, T.; Jurchescu, O. D. The Influence of Isomer Purity on Trap States and Performance of Organic Thin-Film Transistors. *Adv. Electron. Mater.* **2017**, *3*, 1600294.
(79) Curtin, I. J.; Blaylock, D. W.; Holmes, R. J. Role of Impurities in Determining the Exciton Diffusion Length in Organic Semiconductors. *Appl. Phys. Lett.* **2016**, *108*, 163301.
(80) Bracher, C.; Yi, H.; Scarratt, N. W.; Masters, R.; Pearson, A. J.; Rodenburg, C.; Iraqi, A.; Lidzey, D. G. The Effect of Residual Palladium Catalyst on the Performance and Stability of PCDTBT:PC70BM Organic Solar Cells. *Org. Electron.* **2015**, *27*, 266−273.
(81) Usluer, Ö.; Abbas, M.; Wantz, G.; Vignau, L.; Hirsch, L.; Grana, E.; Brochon, C.; Cloutet, E.; Hadziioannou, G. Metal Residues in Semiconducting Polymers: Impact on the Performance of Organic Electronic Devices. *ACS Macro Lett.* **2014**, *3*, 1134−1138.
(82) Koch, F. P. V.; Rivnay, J.; Foster, S.; Müller, C.; Downing, J. M.; Buchaca-Domingo, E.; Westacott, P.; Yu, L.; Yuan, M.; Baklar, M.; Fei, Z.; Luscombe, C.; McLachlan, M. A.; Heeney, M.; Rumbles, G.; Silva, C.; Salleo, A.; Nelson, J.; Smith, P.; Stingelin, N. The Impact of Molecular Weight on Microstructure and Charge Transport in Semicrystalline Polymer Semiconductors−Poly(3-hexylthiophene), A Model Study. *Prog. Polym. Sci.* **2013**, *38*, 1978−1989.
(83) Heinze, J.; Frontana-Uribe, B. A.; Ludwigs, S. Electrochemistry of Conducting Polymers—Persistent Models and New Concepts. *Chem. Rev.* **2010**, *110*, 4724−4771.
(84) Apperloo, J. J.; Janssen, R. A. J.; Nielsen, M. M.; Bechgaard, K. Doping in Solution as an Order-Inducing Tool Prior to Film Formation of Regio-Irregular Polyalkylthiophenes. *Adv. Mater.* **2000**, *12*, 1594−1597.
(85) Heimel, G. The Optical Signature of Charges in Conjugated Polymers. *ACS Cent. Sci.* **2016**, *2*, 309−315.
(86) Scholes, D. T.; Yee, P. Y.; Lindemuth, J. R.; Kang, H.; Onorato, J.; Ghosh, R.; Luscombe, C. K.; Spano, F. C.; Tolbert, S. H.; Schwartz, B. J. The Effects of Crystallinity on Charge Transport and the Structure of Sequentially Processed F4TCNQ-Doped Conjugated Polymer Films. *Adv. Funct. Mater.* **2017**, *27*, 1702654.
(87) Leclerc, M.; Fréchette, M.; Bergeron, J.-Y.; Ranger, M.; Lévesque, I.; Faïd, K. Chromic Phenomena in Neutral Polythiophene Derivatives. *Macromol. Chem. Phys.* **1996**, *197*, 2077−2087.
(88) Leclerc, M. Optical and Electrochemical Transducers Based on Functionalized Conjugated Polymers. *Adv. Mater.* **1999**, *11*, 1491−1498.
(89) Hassab, S.; Shen, D. E.; Österholm, A. M.; Da Rocha, M.; Song, G.; Alesanco, Y.; Viñuales, A.; Rougier, A.; Reynolds, J. R.; Padilla, J. A New Standard Method to Calculate Electrochromic Switching Time. *Sol. Energy Mater. Sol. Cells* **2018**, *185*, 54−60.
(90) Brown, P. J.; Thomas, D. S.; Köhler, A.; Wilson, J. S.; Kim, J.-S.; Ramsdale, C. M.; Sirringhaus, H.; Friend, R. H. Effect of Interchain Interactions on the Absorption and Emission of Poly(3-hexylthiophene). *Phys. Rev. B: Condens. Matter Mater. Phys.* **2003**, *67*, 064203.
(91) Österholm, A. M.; Ponder, J. F.; De Keersmaecker, M.; Shen, D. E.; Reynolds, J. R. Disentangling Redox Properties and Capacitance in Solution-Processed Conjugated Polymers. *Chem. Mater.* **2019**, *31*, 2971−2982.

https://dx.doi.org/10.1021/acs.macromol.0c02719
Macromolecules 2021, 54, 1677−1692